OAK RIDGE NATIONAL LABORATORY LIBRARIES
3 4456 0592210 6

[redacted]

RECEIVED MAY 9 1969

ORNL-4392
UC-41 – Health and Safety

WALKER BRANCH WATERSHED PROJECT: HYDROLOGIC ANALYSIS AND DATA PROCESSING

W. M. Snyder
J. W. Curlin

Oak Ridge National Laboratory
Research Library
4500N, MS-6191
LIBRARY LOAN COPY
DO NOT TRANSFER TO ANOTHER PERSON.
If you wish someone else to see this report, send in name with report and the library will arrange a loan.
ORNL 118(10-05)

OAK RIDGE NATIONAL LABORATORY
operated by
UNION CARBIDE CORPORATION
for the
U.S. ATOMIC ENERGY COMMISSION

Oak Ridge National Laboratory
Research Libraries

Printed in the United States of America. Available from Clearinghouse for Federal Scientific and Technical Information, National Bureau of Standards, U.S. Department of Commerce, Springfield, Virginia 22151
Price: Printed Copy $3.00; Microfiche $0.65

LEGAL NOTICE

This report was prepared as an account of Government sponsored work. Neither the United States, nor the Commission, nor any person acting on behalf of the Commission:

A. Makes any warranty or representation, expressed or implied, with respect to the accuracy, completeness, or usefulness of the information contained in this report, or that the use of any information, apparatus, method, or process disclosed in this report may not infringe privately owned rights; or

B. Assumes any liabilities with respect to the use of, or for damages resulting from the use of any information, apparatus, method, or process disclosed in this report.

As used in the above, "person acting on behalf of the Commission" includes any employee or contractor of the Commission, or employee of such contractor, to the extent that such employee or contractor of the Commission, or employee of such contractor prepares, disseminates, or provides access to, any information pursuant to his employment or contract with the Commission, or his employment with such contractor.

ORNL-4392

Contract No. W-7405-eng-26

Radiation Ecology Section, Health Physics Division

WALKER BRANCH WATERSHED PROJECT: HYDROLOGIC ANALYSIS AND DATA PROCESSING

W. M. Snyder and J. W. Curlin

APRIL 1969

OAK RIDGE NATIONAL LABORATORY
Oak Ridge, Tennessee
operated by
UNION CARBIDE CORPORATION
for the
U.S. ATOMIC ENERGY COMMISSION

OAK RIDGE NATIONAL LABORATORY LIBRARIES

3 4456 0592210 6

CONTENTS

Page

Introduction 1

Basic Data Processing 2

Gage-tape to Card Data Conversion 2

Rainfall Data Editing and Reduction 3

Streamflow Data Editing and Reduction 3

Basic Rainfall Tabulation 4

Definition and Detection of Storms 6

Bounding Parameters for Walker Branch Watershed 9

Streamflow Tabulation 10

Hydrograph Analysis 12

Storm Occurrences 12

Isolation of Stream Response 12

Evaluation of Antecedent Recession 13

Graphical Description of Recession Function 16

Volume of Storm Response 19

Separation of Complex Storms 20

Definition of Rainfall Excess 24

Time Distribution of Rainfall Excess 24

Formulation of a Watershed Intake Function 25

Computation of Distributed Rainfall Excess 28

Example of Calculation of Rainfall Excess 29

Watershed Transfer Function 31

Inflow-Outflow Computation 33

Form of the Transfer Function 35

Page

Analytical Transformation of the Transfer Function . . . 39

Solution for the Linear-Segmented Hydrograph 41

Time-Separated Hydrographs 44

Partially Re-constructed Hydrographs 45

Examples of Time Separated Hydrographs 46

Specific Transfer Functions for Walker Branch Watersheds . . 49

Storm Scales 50

Linearization of Transfer Function 52

Data Manipulation 52

WALKER BRANCH WATERSHED PROJECT: HYDROLOGIC ANALYSIS AND DATA PROCESSING

W. M. Snyder[1] and J. W. Curlin

INTRODUCTION

This report describes the various steps in processing data from continuously recording instruments on the Walker Branch Watershed. The objectives and organization of the Walker Branch Project are outlined in ORNL-TM-2271 (1) and the data processing described herein is aimed at accomplishing those objectives. Processing, as referred to here, means all steps beginning with conversion of raw data from instrument tapes to computer-compatible forms and ending with summaries or analyses which provide input data for mathematical models of watershed ecosystems.

Initial emphasis is on processing of recorded rainfall and streamflow records, with particular treatment of the natural input event, defined here as a storm. Also included, however, are basic tabulations of rainfall and runoff which will form continuous sequential inventories of the water resources of the subwatersheds. As processing and analytical methods undergo continued development, we intend to add inventories and analyses of long-term effects of base-flow on water yield of the streams and to include chemical, biological, and mineralogical inputs-outputs of the streams.

All processing methods are developed under the criterion that the resulting hydrologic data must be of sufficient precision to detect responses to experimental watershed treatments or manipulations. At the same time it is fully recognized that hydrology is essentially a science

[1]Professor of Civil Engineering, Georgia Institute of Technology, Atlanta, Georgia.

of measurement and observation of historical data, and consequently analytical methodologies are statistically rather then deterministically oriented.

BASIC DATA PROCESSING

Five automatic Fischer and Porter[2] (F & P) Series 1548 weighing precipitation digital recorders provide a continuous rainfall record within a triangular network superimposed over the watershed. Streamflow is digitally recorded on F & P model 1542 water level recorders. Data are recorded on paper binary-coded, foil-backed paper tape at 5-minute punch intervals. The precipitation gages resolve rainfall increments of 0.1 in. and are sensitive to changes of 0.025 in. of precipitation. The stage height recorders can sense a change of 0.001 ft. Data from the instruments are processed monthly.

Gage-tape to Card Data Conversion

The conversion of data from 16-channel, binary-coded, punched paper tape to punched card form compatible with an IBM 360 computer system is done on an F & P automatic translator and time-date sequencer. Translation is performed at the Coweeta Hydrologic Laboratory of the U.S. Forest Service, Franklin, North Carolina under interagency agreement with the AEC.

The punched cards are returned to the ORNL Radiation Ecology Section without editing where the cards are then listed, edited, corrected and subsequently processed at the Computer Technology Center.

---

[2]Manufactured by Fischer and Porter Company, Warminster, Pennsylvania 18974.

Rainfall Data Editing and Reduction

The raw rainfall records must be examined for obvious instrumental errors or instrument failure. Also, a preponderant number of the observations at 5-minute intervals will show no rainfall. Data from the corrected deck are, therefore, read into the computer and processed by a program which deletes all zero-data punches. Simultaneously, each retained data point is indexed by time measured from midnight (00:00) of the first day of the month. These data are then punched into a new deck which is greatly reduced by elimination of zero punches. The reduced deck contains one month's data for each of 5 precipitation gages and is preserved for subsequent analysis.

Streamflow Data Editing and Reduction

The editing of raw data from the stage-height recorders is handled similar to the precipitation data. Streamflow records are continuous, however, and do not contain the extent of redundant zero records characteristic of precipitation data. Data reduction for stage-height records is accomplished by retaining time-head readings at sliding intervals. Data are retained at 5-minute intervals for storms of short duration during periods of stream-rise. For longer duration storms the retention interval is expanded until long duration storms and non-storm periods reach a maximum retention interval of 160 minutes. Data analysis is also based on this sliding interval. The single exception is for very long storms with durations $\geqq$ 64 hours; their analyses are based on data at 320-minute intervals. Further discussion of retention intervals is found in the section on Definition and Detection of Storms.

Basic Rainfall Tabulation

Monthly precipitation from the edited and reduced data is summarized and listed sequentially. Figure 1 is a prototype listing which consists of:

(A) Daily precipitation values at each gage in English and metric units.

(B) Weekly rainfall summaries for each gage. Weeks are numbered consecutively beginning January 1.

(C) Monthly totals at each gage.

(D) Weighted monthly totals for each subwatershed. Values weighted by the Thiessen method.

(E) Number of days with rain at each precipitation gage.

(F) Date of occurrence, amount of precipitation, and duration of the storms identified with the procedure outlined in the following section on Definition and Detection of Storms.

(G) Area weighted storm averages by subwatersheds using the Thiessen weighting technique.

(H) Classification and frequency of storms by class and subwatershed.

In addition to the elements shown above the program computes and lists sums of squares (ΣX_i^2) and sums of cross products ($\Sigma X_i X_j$) for subsequent intergage correlations. Continuity of storm identification is maintained by processing two adjacent months contiguously so that storms originating in one month and continuing into the next month will be identified as a single storm rather than two separate events.

PRECIPITATION IN INCHES FOR 10/68

DATE	GAGE NUMBER 1	2	3	4	5
1	0.0	0.0	0.0	0.0	0.0
2	0.2	0.2	0.2	0.2	0.2
3	0.9	0.9	0.8	0.8	0.9
4	0.0	0.0	0.0	0.0	0.0
5	0.0	0.0	0.0	0.0	0.0
6	1.0	1.0	1.0	1.0	1.1
7	0.0	0.0	0.0	0.0	0.0
8	0.0	0.0	0.0	0.0	0.0
9	0.0	0.0	0.0	0.0	0.0
10	0.1	0.1	0.1	0.1	0.1
11	0.0	0.0	0.0	0.0	0.0
12	0.0	0.0	0.0	0.0	0.0
13	0.0	0.0	0.0	0.0	0.0
14	0.0	0.0	0.0	0.3	0.0
15	0.0	0.0	0.0	0.0	0.0
16	0.0	0.0	0.0	0.0	0.0
17	0.0	0.0	0.0	0.0	0.0
18	0.9	0.9	0.9	0.0	1.0
19	0.0	0.0	0.1	0.0	0.0
20	0.0	0.0	0.0	1.0	0.0
21	0.0	0.0	0.0	0.0	0.0
22	0.0	0.0	0.0	0.0	0.0
23	0.0	0.0	0.0	0.0	0.0
24	0.0	0.0	0.0	0.1	0.0
25	0.0	0.0	0.0	0.0	0.0
26	0.0	0.0	0.1	0.0	0.0
27	0.1	0.1	0.1	0.0	0.1
28	0.0	0.0	0.0	0.1	0.0
29	0.0	0.0	0.0	0.0	0.0
30	0.0	0.0	0.0	0.0	0.1
31	0.0	0.0	0.0	0.0	0.0
WEEKLY SUBTOTALS					
40	2.1	2.1	2.0	2.0	2.2
41	0.1	0.1	0.1	0.1	0.1
42	0.9	0.9	1.0	1.8	1.0
43	0.1	0.1	0.2	0.1	0.1
TOTAL	3.2	3.2	3.3	4.1	3.5

(A)

(B)

(C)

AREA WEIGHTED TOTALS
EAST BRANCH 3.5
WEST BRANCH 3.3

(D)

NUMBER OF DAYS WITH RAIN
6 6 8 8 7

(E)

PRECIPITATION IN MILLIMETERS FOR 10/68

DATE	GAGE NUMBER 1	2	3	4	5
1	0.0	0.0	0.0	0.0	0.0
2	5.1	5.1	5.1	5.1	5.1
3	22.9	22.9	20.3	20.3	22.9
4	0.0	0.0	0.0	0.0	0.0
5	0.0	0.0	0.0	0.0	0.0
6	25.4	25.4	25.4	25.4	27.9
7	0.0	0.0	0.0	0.0	0.0
8	0.0	0.0	0.0	0.0	0.0
9	0.0	0.0	0.0	0.0	0.0
10	2.5	2.5	2.5	2.5	2.5
11	0.0	0.0	0.0	0.0	0.0
12	0.0	0.0	0.0	0.0	0.0
13	0.0	0.0	0.0	0.0	0.0
14	0.0	0.0	0.0	20.3	0.0
15	0.0	0.0	0.0	0.0	0.0
16	0.0	0.0	0.0	0.0	0.0
17	0.0	0.0	0.0	0.0	0.0
18	22.9	22.9	22.9	0.0	25.4
19	0.0	0.0	2.5	0.0	0.0
20	0.0	0.0	0.0	25.4	0.0
21	0.0	0.0	0.0	0.0	0.0
22	0.0	0.0	0.0	0.0	0.0
23	0.0	0.0	0.0	0.0	0.0
24	0.0	0.0	0.0	2.5	0.0
25	0.0	0.0	0.0	0.0	0.0
26	0.0	0.0	2.5	0.0	0.0
27	2.5	2.5	2.5	0.0	2.5
28	0.0	0.0	0.0	2.5	0.0
29	0.0	0.0	0.0	0.0	0.0
30	0.0	0.0	0.0	0.0	2.5
31	0.0	0.0	0.0	0.0	0.0
WEEKLY SUBTOTALS					
40	53.3	53.3	50.8	50.8	55.9
41	2.5	2.5	2.5	2.5	2.5
42	22.9	22.9	25.4	45.7	25.4
43	2.5	2.5	5.1	2.5	2.5
TOTAL	81.3	81.3	83.8	104.1	88.9

AREA WEIGHTED TOTALS
EAST BRANCH 89.2
WEST BRANCH 82.9

NUMBER OF DAYS WITH RAIN
6 6 8 8 7

WALKER BRANCH STORM PRECIPITATION FOR 10/68
PRECIPITATION IN INCHES

(F)

STORM DATE	DURATION IN HOURS / GAGE 1 PR.	1 DUR.	2 PR.	2 DUR.	3 PR.	3 DUR.	4 PR.	4 DUR.	5 PR.	5 DUR.
3	0.7	3.8	0.7	3.8	0.7	5.7	0.7	3.2	0.8	3.4
6	0.7	6.3	0.7	6.3	0.7	7.8	0.8	7.2	0.7	6.3
18	0.8	7.4	0.8	7.4	0.8	7.7	0.0	0.0	0.9	11.8
20	0.0	0.0	0.0	0.0	0.0	0.0	0.8	5.5	0.0	0.0
TOTALS	2.2	17.6	2.2	17.6	2.2	21.2	2.3	15.9	2.4	21.6

(G)

AREA WEIGHTED AVERAGES	E. BRANCH PR.	E. BRANCH DUR.	W. BRANCH PR.	W. BRANCH DUR.
	0.7	4.6	0.7	4.4
	0.7	7.3	0.7	6.8
	0.7	7.1	0.8	7.5
	0.2	1.1	0.0	0.0
	2.3	20.1	2.2	18.6

(H)

NUMBER OF STORMS BY CLASSES

CLASS UPPER LIMIT, AREA WTD. PRECIPITATION								
INCHES	0.5	1.0	1.5	2.0	3.0	4.0	5.0	6.0
MILLIMETERS	13.0	25.0	38.0	51.0	76.0	102.0	127.0	152.0
W. BRANCH TOTAL	0	3	0	0	0	0	0	0
E. BRANCH TOTAL	1	3	0	0	0	0	0	0

Fig. 1. Example of Computer Output from Storm Identification and Precipitation Summary Program.

Definition and Detection of Storms

The natural unit of rainfall input to a drainage area is termed a storm occurrence. No rigorous definition is possible for distinguishing between significant amounts and intensities of rainfall which constitute a storm, and insignificant amounts of no consequence to input-output analysis of short-term events. However, it is essential that definitions be established which can be applied in a systematic and unvarying manner to all rainfall records. Such definitions will allow preparation of storm lists unbiased by subjective selection criteria. If the definition is converted to a numeric algorithm, the storm list can be prepared as a step in the routine, sequential processing of the hydrologic data. This implies that a storm will be defined on the basis of precipitation events on the watershed, rather than on the basis of positive and detectable stream response to some rainfall input. Since rainfall is the causal factor it is rational that storms be identified from precipitation events rather than streamflow phenomena. When storms are defined on the basis of input rainfall they are not subject to definitional differences caused by variation in the ability of the watershed to absorb and retain water, or by varying rates excess water is released to streamflow.

Figure 2 shows the schematic diagram of the storm decision algorithm. This algorithm detects storms when rainfall rates or volume in the precipitation records exceed certain minima. It is specifically designed to make sequential "storm" or "no-storm" decisions on each rain occurrence without the need for multiple passes over the data. The diagram consists essentially of two bounding lines on a graph of accumulated rainfall versus time.

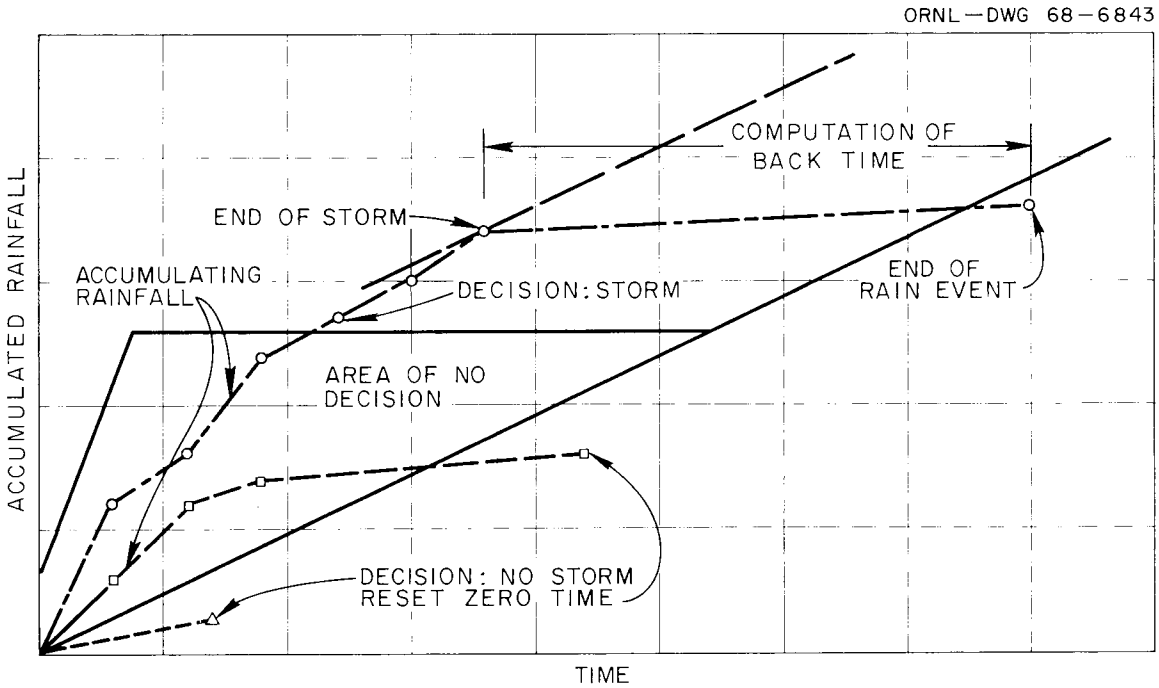

Fig. 2. Mechanics of the Sequential Decision Algorithm Used for Storm - No-Storm Decisions.

Each rainfall event is examined in the computer by evaluating the total, or accumulated depth of rain which has fallen between some arbitrary beginning time and the time of check. If the total depth for the elapsed time lies below the lower bounding line, the rain occurrence is declared no-storm and zero time is advanced to the next rainfall occurrence. For a recording interval of five minutes this means that zero time advances in 5-minute steps if rain is occurring at rates less than the slope of the lower bounding line. However, if the sensitivity increment of the digital raingage divided by 5 minutes is greater than the slope of the lower line, this lower line is not effective. For example, if the increment of rainfall proceeds in step of 0.1 in., the lower line must have a slope in excess of 0.1 in./5 min or 1.2 in./hr for the lower bounding line to be effective in declaring an immediate decision no storm. The lower line also serves other purposes which will be discussed later.

If the locus of points of cumulative rainfall versus elapsed time crosses upward over the lower bounding line, the zero time does not advance. So long as the locus lies between the lower and upper bounding lines the decision to declare the rainfall occurrences as storm or no-storm is postponed. Eventually either of two possibilities must happen. When the rain stops the locus becomes horizontal (zero slope) as time advances to the right. The locus must, therefore, either cross the lower bound, or else climb upward across the upper bound. If the former happens, the rain is declared no-storm. If the latter happens, the rain is declared a storm.

It is necessary to define two properties of rain occurrence, 1) the total depth which fell and 2) the time from beginning to end of rain known as duration of rainfall. Definition of both these properties depends upon identifying the end of rain occurrence.

When some period without rain follows a storm rainfall period, the accumulating locus on the graph is horizontal. If this period without rain is of sufficient length, the locus will cross the lower bounding line. When this happens an end of the storm has occurred. However, because of irregular time intervals the actual end of rain is not known.

To compute the end of the storm the time when the storm locus crosses the lower bounding curve is first flagged. Increments of time are then counted backwards in the record until a point is found where the (negative) slope of the locus is again greater than the slope of the lower bounding line. The beginning (counting backward in time) is the interval where this slope exceedance first occurs in the end of the storm. The accumulated rainfall from the beginning of the storm to that point is the storm rainfall, and the elapsed time from zero to that point is the storm duration.

The date, beginning time, total rainfall, and duration of rain for each event are noted and printed on the Storm Table listings for each month (Fig. 1).

Bounding Parameters for Walker Branch Watershed

The values describing the bounding lines in Fig. 2 for the Walker Branch Watershed were chosen initially as follows: The lower bounding line is expressed by the equation

$RSC = 0.05\ \Delta T$

where ΔT is hours from zero-time

0.05 is in. per hr

and RSC is subcritical rainfall in in.

Any rain $\leqq$ RSC is rejected as a storm.

The segments of the upper bounding line are defined as

$RC = 0.2 + 0.1\ \Delta T$ for $\Delta T \leqq 3$

$RC = 0.5$ for $3 < \Delta T \leqq 9$

$RC = 0.05 + 0.05\ \Delta T$ for $< \Delta T$

where RC is critical rainfall in in. Any rain $\geqq$ RC at any time during a rainfall event is declared a storm for purposes of further data processing and analysis.

Streamflow Tabulations

Streamflow summaries (Fig. 3) are organized on a format similar to the rainfall tabulations described earlier. Listings consist of the following elements.

(A) Average daily discharge in cfs for each subwatershed.

(B) Total daily flow volume in cu ft.

(C) Parallel output of discharge as in (A) expressed in metric units cms.

(D) Total daily flow similar to (B) expressed in cu M.

(E) Monthly totals for volumes and average flow rates.

(F) Weekly totals for volumes and average flow rates.

(G) Maximum and minimum flows for each storm.

(H) Flow duration table showing number of day flow is in selected flow range.

DAILY FLOWFOR 10/68

	EAST BRANCH				WEST BRANCH				
DATE	(A) DISCHARGE CFS	(B) VOLUME CU.FT.	(C) DISCHARGE CMS	(D) VOLUME CU.M.	DATE	DISCHARGE CFS	VOLUME CU.FT.	DISCHARGE CMS	VOLUME CU.M.
1	1.3956E-02	1.2058E 03	3.9520E-04	3.4145E 01	1	1.9439E-01	1.6795E 04	5.5044E-03	4.7558E 02
2	1.2953E-02	1.1192E 03	3.6680E-04	3.1692E 01	2	1.9439E-01	1.6795E 04	5.5044E-03	4.7558E 02
3	3.3135E-02	2.8628E 03	9.3828E-04	8.1067E 01	3	2.1200E-01	1.8317E 04	6.0033E-03	5.1869E 02
4	2.7943E-02	2.4143E 03	7.9127E-04	6.8366E 01	4	1.9038E-01	1.6449E 04	5.3909E-03	4.6577E 02
5	2.2377E-02	1.9334E 03	6.3366E-04	5.4748E 01	5	1.8102E-01	1.5640E 04	5.1259E-03	4.4288E 02
6	3.1171E-02	2.6931E 03	8.8266E-04	7.6261E 01	6	2.0111E-01	1.7376E 04	5.6947E-03	4.9202E 02
7	4.9070E-02	4.2397E 03	1.3895E-03	1.2005E 02	7	1.9334E-01	1.6704E 04	5.4747E-03	4.7302E 02
8	3.2763E-02	2.8307E 03	9.2774E-04	8.0157E 01	8	1.8932E-01	1.6357E 04	5.3609E-03	4.6318E 02
9	2.6859E-02	2.3206E 03	7.6057E-04	6.5714E 01	9	1.8932E-01	1.6357E 04	5.3609E-03	4.6318E 02
10	2.5127E-02	2.1709E 03	7.1151E-04	6.1474E 01	10	1.8932E-01	1.6357E 04	5.3609E-03	4.6318E 02
11	2.4773E-02	2.1403E 03	7.0148E-04	6.0608E 01	11	1.8932E-01	1.6357E 04	5.3609E-03	4.6318E 02
12	2.3980E-02	2.0719E 03	6.7904E-04	5.8669E 01	12	1.8932E-01	1.6357E 04	5.3609E-03	4.6318E 02
13	2.2710E-02	1.9621E 03	6.4307E-04	5.5562E 01	13	1.8932E-01	1.6357E 04	5.3609E-03	4.6318E 02
14	2.1113E-02	1.8242E 03	5.9787E-04	5.1656E 01	14	1.8932E-01	1.6357E 04	5.3609E-03	4.6318E 02
15	2.0794E-02	1.7966E 03	5.8882E-04	5.0874E 01	15	1.8932E-01	1.6357E 04	5.3609E-03	4.6318E 02
16	2.1086E-02	1.8218E 03	5.9709E-04	5.1589E 01	16	1.8932E-01	1.6357E 04	5.3609E-03	4.6318E 02
17	2.6536E-02	2.2927E 03	7.5141E-04	6.4922E 01	17	1.8821E-01	1.6261E 04	5.3295E-03	4.6047E 02
18	4.3611E-02	3.7680E 03	1.2349E-03	1.0670E 02	18	2.0266E-01	1.7510E 04	5.7387E-03	4.9583E 02
19	5.8174E-02	5.0263E 03	1.6473E-03	1.4233E 02	19	2.0083E-01	1.7351E 04	5.6868E-03	4.9134E 02
20	3.8370E-02	3.3152E 03	1.0865E-03	9.3875E 01	20	1.9247E-01	1.6630E 04	5.4503E-03	4.7090E 02
21	3.2287E-02	2.7896E 03	9.1427E-04	7.8993E 01	21	1.8764E-01	1.6212E 04	5.3134E-03	4.5907E 02
22	3.1674E-02	2.7367E 03	8.9693E-04	7.7494E 01	22	1.8764E-01	1.6212E 04	5.3134E-03	4.5907E 02
23	3.1674E-02	2.7367E 03	8.9693E-04	7.7494E 01	23	1.8764E-01	1.6212E 04	5.3134E-03	4.5907E 02
24	3.6129E-02	3.1215E 03	1.0231E-03	8.8392E 01	24	1.8764E-01	1.6212E 04	5.3134E-03	4.5907E 02
25	3.7967E-02	3.2804E 03	1.0751E-03	9.2891E 01	25	1.8764E-01	1.6212E 04	5.3134E-03	4.5907E 02
26	2.9402E-02	2.5403E 03	8.3257E-04	7.1934E 01	26	1.8764E-01	1.6212E 04	5.3134E-03	4.5907E 02
27	3.2552E-02	2.8125E 03	9.2179E-04	7.9642E 01	27	1.8764E-01	1.6212E 04	5.3134E-03	4.5907E 02
28	3.9361E-02	3.4008E 03	1.1146E-03	9.6300E 01	28	1.8035E-01	1.5582E 04	5.1069E-03	4.4123E 02
29	2.8881E-02	2.4953E 03	8.1783E-04	7.0660E 01	29	1.7136E-01	1.4806E 04	4.8524E-03	4.1925E 02
30	2.8580E-02	2.4693E 03	8.0930E-04	6.9923E 01	30	1.7136E-01	1.4806E 04	4.8524E-03	4.1925E 02
31	2.9392E-02	2.5395E 03	8.3230E-04	7.1911E 01	31	1.7136E-01	1.4806E 04	4.8524E-03	4.1925E 02
AVG	3.0142E-02		8.5353E-04		(E) AVG	1.8911E-01		5.3551E-03	
TOTAL		8.0732E 04		2.2861E 03	TOTAL		5.0652E 05		1.4343E 04

AVERAGE WEEKLY FLOW

WEEK					WEEK				
40	2.2469E-02	1.9414E 03	6.3626E-04	5.4973E 01	40	1.9538E-01	1.6881E 04	5.5326E-03	4.7802E 02
41	2.9326E-02	2.5338E 03	8.3042E-04	7.1748E 01	(F) 41	1.8989E-01	1.6407E 04	5.3771E-03	4.6458E 02
42	3.2812E-02	2.8350E 03	9.2914E-04	8.0278E 01	42	1.9316E-01	1.6689E 04	5.4697E-03	4.7258E 02
43	3.3098E-02	2.8597E 03	9.3724E-04	8.0977E 01	43	1.8764E-01	1.6212E 04	5.3134E-03	4.5907E 02

STREAM FLOW SUMMARY FOR 10/68

(G) MAXIMUM/MINIMUM FLOW READINGS

EAST BRANCH					WEST BRANCH				
STORM DATE	MAXIMUM CFS	MAXIMUM CMS	MINIMUM CFS	MINIMUM CMS	STORM DATE	MAXIMUM CFS	MAXIMUM CMS	MINIMUM CFS	MINIMUM CMS
3	5.6951E-02	1.6127E-03	1.3189E-02	3.7348E-04	3	2.8463E-01	8.0597E-03	1.8103E-01	5.1262E-03
6	5.6951E-02	1.6127E-03	2.1252E-02	6.0178E-04	6	2.4570E-01	6.9575E-03	1.8103E-01	5.1262E-03
18	6.8284E-02	1.9336E-03	2.8838E-02	8.1660E-04	18	2.3032E-01	6.5218E-03	1.8764E-01	5.3135E-03
20	4.1835E-02	1.1846E-03	3.1675E-02	8.9694E-04	20	0.0	0.0	0.0	0.0
MONTHLY	6.8284E-02	1.9336E-03	1.2505E-02	3.5411E-04	MONTHLY	2.8463E-01	8.0597E-03	1.7137E-01	4.8527E-03

TOTAL VOLUME BY STORM

EAST BRANCH			WEST BRANCH		
STORM DATE	CU.FT.	CU.M.	STORM DATE	CU.FT.	CU.M.
3	4.8111E 03	1.3623E 02	3	2.8656E 04	8.1144E 02
6	5.2615E 03	1.4899E 02	6	2.8666E 04	8.1173E 02
18	6.5017E 03	1.8411E 02	18	2.8865E 04	8.1738E 02
20	4.8196E 03	1.3648E 02	20	0.0	0.0

(H) NUMBER OF DAYS BY FLOW CLASSES IN CFS

UPPER LIMIT	0.1	0.2	0.3	0.4	0.5	1.0	1.5	5.0
EAST BRANCH	31	0	0	0	0	0	0	0
WEST BRANCH	0	27	4	0	0	0	0	0

Fig. 3. Example of Computer Output from Streamflow Summary Program.

HYDROGRAPH ANALYSIS

Hydrograph analysis is the investigation of the relationship between storm rainfall and the response in streamflow. Two elements of streamflow must be considered, 1) the volume of streamflow in relation to the volume of rainfall, and 2) the temporary storage and release of this excess rainfall to form streamflow. Hydrograph analysis is thus the determination of short-time response of the stream.

Storm Occurrences

The determination of dates, beginning times, total rainfall, and duration of storm occurrences is described in the section on "Definition and Detection of Storms", p. 6. A storm occurrence is determined for either subwatershed whenever a storm occurs by rainfall definition at any raingage which contributes weighted rainfall to that subwatershed.

Isolation of Stream Response

During intervals without significant rainfall streamflow gradually decreases. This stream regimen is known as a "recession" to lesser streamflow rates. When the stream responds to an input of rainfall sufficient to overcome initial wetting requirements, the flow rate exceeds the "recession" rate established prior to the storm. In terms of the streamflow hydrograph, the total response of the stream is that discharge in excess of the antecedent recession.

The hydrograph is a graph of discharge versus time. The integrated area on a hydrograph is expressible as discharge multiplied by time, which is a volume. Mathematically, the integration of discharge across a period of time produces volume of runoff. The volume of storm flow observed in

the stream must thus be determined by integration, or a summation of flow rates. The proper volume of flow must, in some manner, be isolated from other non-storm streamflow.

Evaluation of Antecedent Recession

Figure 4 shows an idealized and simplified response of a stream to an occurrence of "storm" rainfall. The observed, or recorded, streamflow is shown by the continuous line. Initial wetting demands (interception, depression storage, and some soil moisture recharge) can be considered satisfied at point (t_3,q_3), beyond this point in time the streamflow increases, crests, then recedes to near pre-storm levels. The volume of streamflow for that particular storm is the area below the continuous line but above some projection of the antecedent recession beneath the current storm response. The projection is shown as a dashed line in Fig. 4. The left hand boundary of the area representing the stream response is the point (t_3,q_3). The right-hand boundary is indefinite. The volume of storm response includes the area under a recession tail which may continue for a long time. Practical hydrograph analysis, on the other hand, demands that some finite ending time of the storm be used. Procedures for establishing a practical ending time and for computation of the volume will be given later.

It is necessary to establish some means of projecting the antecedent recession forward through point (t_3,q_3) and beneath the current storm. Essentially, this amounts to fitting some mathematical function to the antecedent recession, and then evaluating this function for times beyond t_3. In Fig. 4 the points (t_1,q_1), (t_2,q_2), and $t_3,q_3)$, represent data points of stored streamflow data. The original data points punched at

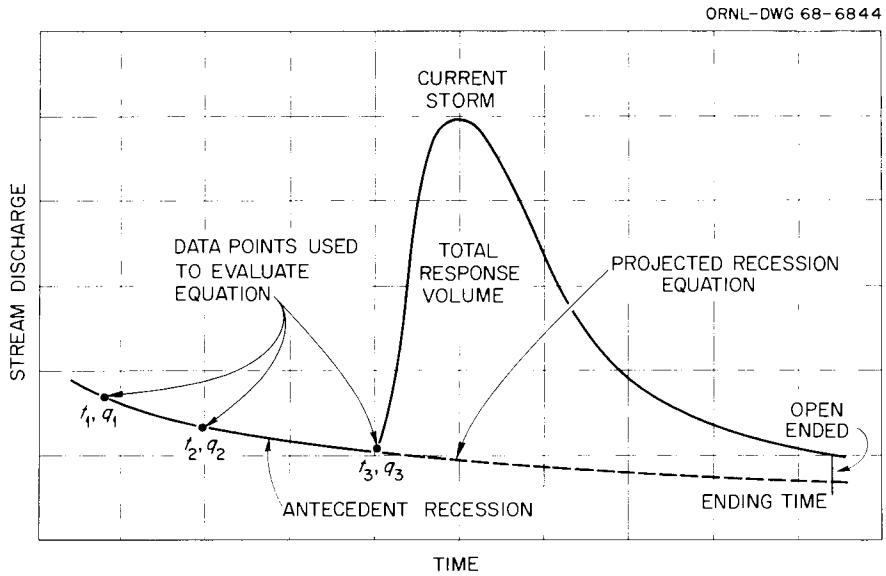

Fig. 4. An Idalized and Simplified Storm Hydrograph Typical of a Stream's Response to a Storm Event.

5-minute intervals were reduced to some lesser number at non-uniform intervals of time as described earlier. The three points shown are from the reduced data set.

The function chosen to project the antecedent recession must possess several properties which can be specified. First, the curve of the function must be made co-locational with the reduced data points antecedent to the storm, one point for each parameter of the function. The curve must, therefore, be easily fitted to such points. Second, the rate of streamflow recession decreases as streamflow approaches some low-flow value. Streamflow should become nearly constant near this low-flow value after a prolonged period of no rainfall. This requires that the function decrease monotonically and become asymptotic to some low value of streamflow.

The mathematical function known as the decreasing exponential has the properties specified above. A form frequently used for streamflow recession is

$$q = a_1 e^{-b_1 t} \tag{1}$$

where q is stream discharge, t is time measured from some initial time, and a_1 and b_1 are constants.

Equation 1 has one scale parameter, a_1, and one shape parameter, b_1. It is desirable for the function to be capable of assuming various shapes. This is accomplished (2) by modifying the function as shown in Eq. 2.

$$q = ae^{-bt^m} \tag{2}$$

The additional shape parameter in Eq. 2 has the effect of transforming the time scale from t to t^m. The constant b controls the recession in

the transformed time t^m and the interplay of the two coefficients allows infinite variability of recession shapes.

If Eq. 2 is modified slightly by a re-definition of time, a simple fitting process can be developed. Without this modification fitting Eq. 2 to the three points (t_1,q_1), (t_2,q_2), and (t_3,q_3) would require solution of three rather difficult simultaneous equations. The modification consists of writing Eq. 2 in the form of Eq. 3.

$$q = ae^{-bT^m} \tag{3}$$

where

$$T = \frac{t - t_1}{t_2 - t_1}$$

This definition forces T to assume the value of zero at time t_1, and the value of unity at time t_2. When T = 0 it can be seen in Eq. 3 that $a = q_1$. When T = 1 it can also be seen that $e^{-b} = q_2/q_1$. At point (t_3,q_3) Eq. 3 takes the form

$$q_3 = q_1 \, (q_2/q_1)^{T_3^m}$$

This equation can be solved for m giving

$$m = \frac{\log \dfrac{\log (q_3/q_1)}{\log (q_2/q_1)}}{\log T_3}$$

With the constants a, b, and m known, Eq. 3 can be projected beneath the hydrograph of stream response of the storm under analysis. This projection extends forward to the ending time.

Graphical Description of Recession Function

The effect of the second shape parameter, m, in Eq. 3 is illustrated in Fig. 5. Three curves are shown which have the points (t_1,q_1) and

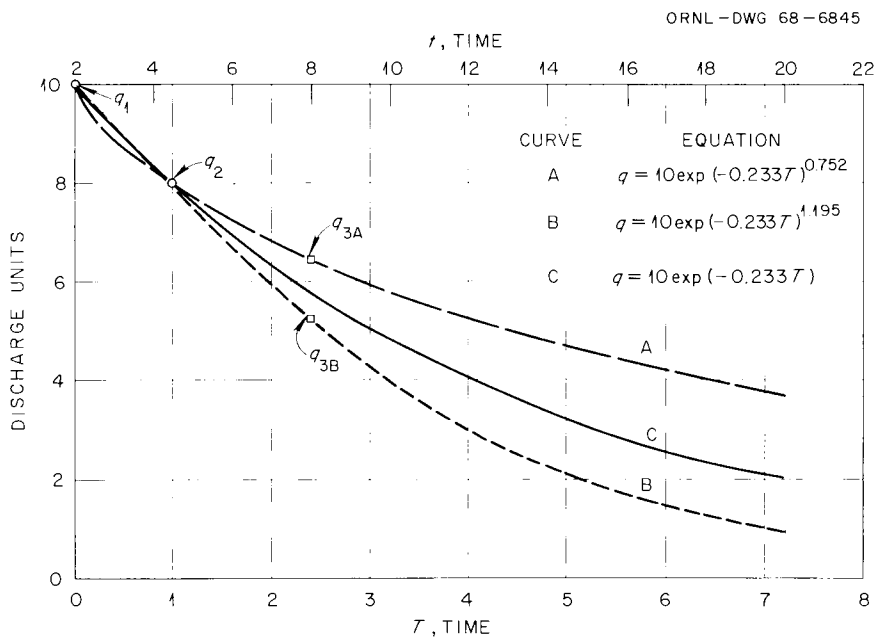

Fig. 5. Effect of the Second Shape Parameter, m, in the Streamflow Recession Function $q = ae^{-bt^m}$.

(t_2, q_2) in common; specifically, the value of q_1 is 10 units, the value of q_2 is 8 units. Therefore, a in Eq. 3 is 10 and e^{-b} is 8/10, so that the value of b can be found to be 0.233.

Curve C in Fig. 5 is of the functional form of Eq. 1. This is the same as Eq. 3 with m = 1. Only the two points (t_1, q_1) and (t_2, q_2) are needed for solution of Eq. 1. Since there is only one shape parameter, b, only one curve can result, and this is the curve C.

When using Eq. 3 an additional point is necessary to evaluate the shape parameter m. Two cases are shown in Fig. 5; Curve A lies above Curve C, and Curve B lies below C. These curves are determined by the requirement that A pass through q_{3A} in addition to q_1 and q_2. In the same manner, Curve B passes through q_{3B}.

The value for m for Curve A is

$$m = \frac{\log \dfrac{\log (6.5/10}{\log (8/10)}}{\log 2.4} = 0.752.$$

The value for m for Curve B is

$$m = \frac{\dfrac{\log (5.3/10)}{\log (8/10)}}{\log 2.4} = 1.195.$$

The effect of the small value of m in Curve A is to "stretch" the recession trend producing a shallow, slowly descending curve. The higher value in Curve B causes a "compression" of the recession trend and consequently steeper descending curve, which, nonetheless, bends and becomes asymptotic to the abscissa.

Volume of Storm Response

The area in Fig. 4 bounded by the curve of the recorded storm hydrograph and the projected recession curve is the volume of water representing the stream response to the rainfall input. If the ordinate, stream discharge, is measured in cfs and the abscissa, time, is measured in sec, then any area on the graph is $(ft^3/sec)(sec) = ft^3$.

It is necessary to compute the total area between the two bounding curves and between point t_3 on the left and some projection of the storm recession on the right. The computation is performed by numeric integration. Beyond the "ending time" an approximating mathematical integral will be used. Numeric integration is necessary for most of the curve since a mathematical function for the upper curve, the recorded storm hydrograph, is not known.

The recorded storm hydrograph actually consists of a series of discrete points. Call these points (t_i, q_i) where the index i will vary from 3 to N. If no recorded data point is located exactly at the ending time the value of q_N can be interpolated linearly between q_{N-1} and the q_{N+1}, the value to the right of the ending time. For each point (t_i, q_i) the projected recession must be evaluated for t_i. Call these recession points a_i. Subtracting the recession ordinates from the streamflow ordinates produces the discrete points $(t_i, q_i - a_i)$ which represent the ordinates of the storm response.

It may be assumed that a straight line connects the ordinates $q_i - a_i$. The incremental area between any two adjacent ordinates is then readily computed. The first incremental area will be $1/2(q_4 - a_4)(t_4 - t_3)$. The second incremental area will be $1/2(q_5 - a_5 + q_4 - a_4)(t_5 - t_4)$. The volume of

storm flow from time t_3 to the "ending time" is the sum of these incremental areas.

Beyond the "ending time" of the storm the volume in the recession tail will be small. It will be sufficient to approximate this value with a definite integral and thus avoid the more time consuming process of numeric integration. The device used for the definite integral is Eq. 3 as evaluated for the antecedent recession. It is assumed that the same recession curve will apply beyond the "ending time."

Call the ending time t_N and the storm ordinate at that time $q_N - a_N$ as indicated above for numeric integration. Then the projected recession is

$$q = (q_N - a_N)e^{-b\left[\frac{t-t_N}{\Delta t}\right]^m} \tag{4}$$

where Δt is $t_2 - t_1$ used in evaluation of the shape parameters for the antecedent recession. If t_N be considered zero time for the projected recession, then Eq. 4 becomes

$$q = (q_N - a_N)e^{-b\left(\frac{t}{\Delta t}\right)^m} \tag{5}$$

The approximate volume of runoff beyond the ending time is the integral (5) of Eq. 5:

$$V = \int_0^\infty q\,dt = (q_N - a_N)\int_0^\infty e^{-b\left(\frac{t}{\Delta t}\right)^m}\,dt$$

$$= \Delta t(q_N - a_N)\frac{1/m!}{b^{1/m}} \tag{6}$$

This volume plus the volume obtained by numeric integration is the total volume of storm runoff in cubic feet.

Separation of Complex Storms

Some provision must be made for separation of the hydrographs of rain events which follow closely upon one another. The definition of storms by

the algorithm in Fig. 2 provides some insurance that most rain events will be separated into a time series of distinct occurrences. However, this cannot be taken as a guarantee that the resulting hydrographs will not overlap in time.

Reference to Fig. 2 shows that there can be no significant rainfall between the points labeled "End of Storm" and "End of Rain Event". If significant rain had occurred the curve of accumulating rainfall would have remained above the lower bounding line and an "End of Rain Event" would not have been detected. This span of time from "End of Storm" to "End of Rain Event" provides the insurance of separation of rain into a series of distinct occurrences. Reference to Fig. 4, however, shows that the time base of the resultant streamflow event extends from the point (t_3, q_3) to the ending time. It is possible for the second of two distinct rain events to occur before the ending time of the hydrograph of the first event. When this happens the hydrograph of streamflow will again begin to rise instead of receding smoothly to the ending time as indicated in Fig. 4.

In a later section of this report it will be seen that the time base of the hydrograph will not be less than four times the duration of the rain event. For this relative time base the open-ended ordinate, as shown in Fig. 4, can be expected to be small. Relatively little volume of runoff will be contained in this recession tail of the storm. Some compromise to compute volumes of runoff for overlapping storms should, therefore, introduce little error into the total storm volume.

The method devised for separating hydrographs of complex storms for the Walker Branch Watershed Project is shown in Fig. 6. In this figure

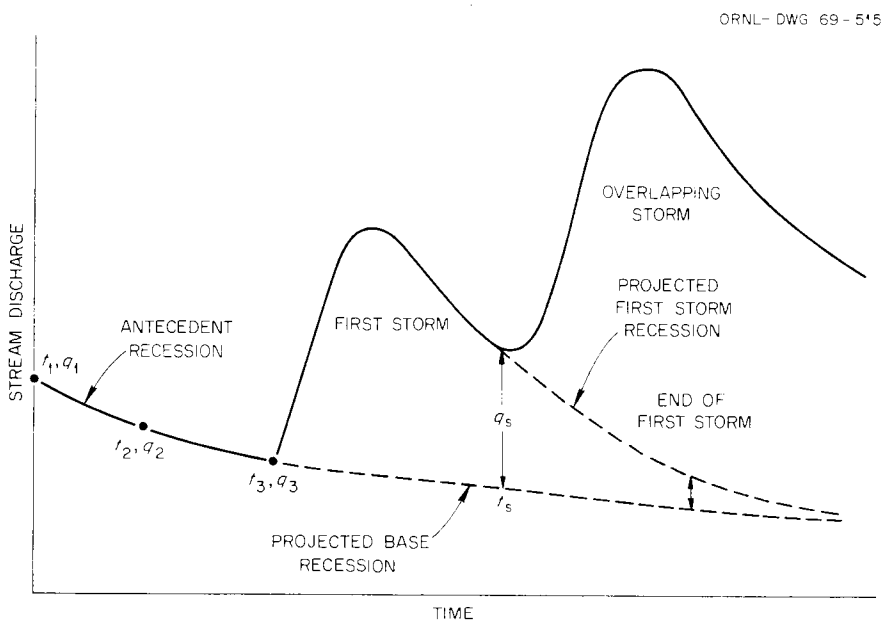

Fig. 6. Separation of Hydrographs from Overlapping Storm Events.

a second storm occurs before the end of the first storm. The start of rise of the second storm takes place at time t_s where the storm ordinate of the first storm is q_s. The recession antecedent to the first storm was evaluated by points (t_1,q_1), (t_2,q_2) and (t_3,q_3) just as in Fig. 4.

It is now assumed that the shape parameters "b" and "m" of recession Eq. 3 as evaluated for the antecedent recession, remain constant for the "first storm recession" in Fig. 6. The "a" of Eq. 3 is the q_1 in Fig. 6, and the time variable "t" of the equation is zero at time t_1. The assumption of constant "b" and "m" produces an equation for the recession of the first storm which has the same shape as the antecedent recession, but which has an initial ordinate q_s instead of q_1, and time zero at t_s.

The volume in the recession of the first storm, beyond the time t_s, can be computed from Eq. 6 by substituting q_s for q_N-a_N.

The ordinates of the recession of the first storm are readily computed from the recession equation. These ordinates can be used in analysis of the hydrograph of the first storm. Additionally, these recession ordinates can be added to the corresponding ordinates of the antecedent recession, and these composite ordinates form a new antecedent recession for the overlapping storm.

In the event a third storm were to occur, overlapping the second storm, the same process can be repeated. It is only necessary to work with the new t_s and q_s for the second overlapping storm. The shape parameters "b" and "m" must be retained since there are no new recessions during a complex storm period which could be used for their reevaluation.

Definition of Rainfall Excess

The volume of storm flow as computed is a consequence of rain falling on the drainage area. However, not all rainfall becomes streamflow. Some rain is intercepted by trees and plants, some wets the surface layers of the soil and evaporates before it can become streamflow. A portion of the water entering the soil profile may percolate downward and pass out of the watershed at deep levels rather than as streamflow. The combined loss from all sources is called "storm loss".

It can be seen, therefore, that storm flow computed by integration of the stream hydrograph, represents an excess of rainfall above some amount which is lost or diverted. The difference between measured storm rainfall and measured storm runoff is the volume of rain lost or diverted. The volume of streamflow and the volume of rainfall excess by this concept are identical. Consequently, the method of computing storm flow has a direct consequence in defining rainfall excess.

The term rainfall excess is used frequently in description of input-output relationships in hydrograph analysis. However, its explicit meaning always depends upon the method of computing storm flow volume. In this report the volume of excess means the volume of total stream response as shown in Fig. 4. This volume includes water which enters the surface layers of the soil, flows downslope, emerges at some point, and enters the stream channel in time to pass the stream gage before the "ending time" of the storm hydrograph.

Time Distribution of Rainfall Excess

In the preceding section the volume of rainfall excess was defined to be the volume of storm flow. It is necessary to distribute this volume

throughout the duration of the storm rainfall. The actual watershed processes by which incoming rainfall divides into retained or diverted amounts and the excess amounts cannot presently be stated in rigorous mathematical form. Soil moisture theory as applied to infiltration at a specific point can be stated. However, the integral of such a point function, across the watershed space, is not possible. Spatial variation of soil characteristics, of initial moisture states, and of rainfall, present insurmountable difficulties. Superimposed on these are difficulties produced by rapid fluctuations in rainfall rate during a storm. Consequently, some approximate but rational method of determining the time distribution of rainfall excess is necessary. This approach will be based on macro-scale processes of the entire watershed rather than the micro-scale processes of point infiltration theory.

Formulation of a Watershed Intake Function

It is known from infiltration theory, and by observation during rainfall, that intake rates into the soil are high when the soil is dry, and lower when the soil becomes wet. Consequently, for a given storm, a watershed can absorb rainfall at extremely high rates when the storm begins, but increasing rates of rainfall excess will develop as the storm progresses. It is also known that the intake rate does not decrease to zero, but stabilizes at some small, asymptotic rate. If the rate at which intake changes is proportional to the present rate, then one can write the differential equation, Eq. 7.

$$df = -K\,(f-f_c)dt \qquad (7)$$

where df is the change in intake rate in time dt, K is a proportionality constant, f is the current intake rate, and f_c is the final rate.

This equation can be integrated. The resulting equation indicates that the intake rate f varies exponentially with time. However, further modification of the equation, and the need for an efficient computational form require instead that the differential be changed to a finite-difference form. This form is given in Eq. 8.

$$f_t - f_{t-1} = -K(f_{t-1} - f_c)\ \Delta t \tag{8}$$

where f_t is the intake at some time t, and f_{t-1} is the intake at $t - \Delta t$. In Eq. 8 it is seen that when K and f_c are known values of the intake rate, f_t can be computed from the rate f_{t-1}. Then f_{t+1} can be computed from f_t and so on for the entire duration of the storm.

Equation 8 is still too limited in form for practical use. For any value $K > 0$ the values of intake would steadily decrease and approach f_c asymptotically. While this is reasonable for periods with continuous moderate rainfall, it is not reasonable for periods of light rain or no rain. During such "breaks" in storm rainfall the potential intake rate should show little change or else increase.

One way of controlling the potential intake rate is to make K in Eq. 8 dependent on the rainfall in each period Δt during the storm. Consider the form in Eq. 9.

$$K = \frac{R_t + f_a - f_{t-1}}{R_t + f_a - f_c} \quad \frac{R_t - f_c}{R_t + f_c} \tag{9}$$

where R_t is rainfall during time Δt, and f_a is an upper limit to the intake rate.

When R_t is large, K will approach 1, and f_t in Eq. 8 will approach f_c. Physically, this means during significant rains the intake rate decreases and approaches the final rate.

When $R_t = f_c$, K is zero and f_t will equal f_{t-1}. This means that when rainfall is equal to the final intake rate there is no change in the current intake rate.

When $R_t = 0$ and f_{t-1} is near f_a, K will be negative and f_t will be larger than f_{t-1} which is nearly f_a. For periods without rain, and with the intake rate high, the rate will approach the maximum rate.

When $R_t = 0$ and f_{t-1} is near f_c, K will approach -1 and f_t will approach $2 f_{t-1} - f_c$. Since f_{t-1} is slightly larger than f_c, f_t will be slightly larger than f_{t-1}. Physically this means the intake rate will recover from the final rate during periods of no rainfall.

If the value for K in Eq. 9 is substituted into Eq. 8, the complete finite difference equation is given by Eq. 10:

$$f_t = f_{t-1} \quad \frac{R_t + f_a - f_{t-1}}{R_t + f_a - f_c} \quad \frac{R_t - f_c}{R_t + f_c} \quad f_{t-1} - f_c \quad \Delta t \qquad (10)$$

In summary, Eq. 10 is a finite difference form for computation of watershed intake rates. The properties for which it was developed are as follows:

1. For periods of moderate rainfall the intake will decrease asymptotically to some final value f_c.
2. For period of rainfall equal to the lower limit f_c the intake rate will not change.
3. For periods of low rainfall the intake rate will increase, drawing away from the lower limit in what may be described as reversed asymptotic.
4. For continued periods with little or no rain the intake rate will approach asymptotically an upper limit f_a.

5. If rain begins when the intake rate is near the upper limit f_a, the intake rate decreases abruptly.

It should be noted that Eq. 10 cannot be readily integrated. Since rainfall, R, is an irregular and unknown function of time, direct integration is not possible. It should be further noted that this equation represents intake for an entire watershed or some areal subportion of a watershed, and is not a "point" function derived from infiltration theory.

Computation of Distributed Rainfall Excess

The watershed intake function presented in the preceding section is descriptive of the potential of the watershed to infiltrate rainfall. It does not mean that infiltration actually takes place at that rate.

If rainfall during some period Δt exceeds the average of the intake function at the beginning and end of Δt, then infiltration will take place at this average rate $(f_t + f_{t-1})/2$. The difference between R_t and $(f_t + f_{t-1})/2$ is the rainfall excess for that period. If rainfall for any period Δt is less than the average of the intake function values, then the actual infiltration rate will be the rainfall rate and no excess will occur.

In order to compute the rainfall excess for all periods of length Δt during a storm occurrence, it is necessary to compute first the watershed intake function during the storm. Following this the periods during which an excess of rain occurs can be identified, the excess computed, and then totaled for all periods of excess. This total of excess must equal the volume of streamflow computed in the section "Volume of Storm Response", p. 19.

It is possible to compute the watershed intake function from Eq. 10 if the watershed physical characteristics, f_a and f_c are known. To start the process, however, some initial value of the function must also be known. It is assumed here that the values of f_a and f_c can be estimated for the watershed. However, no method is known for direct determination of the initial value, consequently it will be computed for each storm by trial and error.

Example of Calculation of Rainfall Excess

Table 1 shows a complete example of rainfall excess calculations. In this example an hour unit of time is used for simplicity. However, any unit can be used provided R, f, f_a, and f_c are scaled to the appropriate time. Also f_t and f_{t-1} are values of the watershed intake function separated by one unit of the time period used.

Specific features should be noted in Table 1. For the first hour, when rainfall was low, the value of the intake function increased from 2.00 to 2.121 in./hr. A similar increase, portraying the recovery of intake capacity, also occurred when rainfall was light at the end of the storm. During the second hour, when rainfall was just equal to the lower limit of f_c, the intake function remained constant at 2.121 in./hr. During the central portion of the storm, when rainfall was high, the intake decreased rapidly, representing reduced soil infiltration rates over the major portion of the watershed.

The average infiltration rate for each period is shown in the next-to-last column. Only during the 8th and 9th hours was rainfall in excess of the average intake rate.

Table 1. Example of Rainfall Excess Computation

Assumed Values: $f_a = 2.40$ in./hr, $f_c = 0.10$ in./hr, $f_0 = 2.00$ in./hr.

All Values in in./hr.

Time hrs	R_t	A^a	B^b	C^c	D^d	$\left(\frac{A}{B}\ \frac{C}{D}\right)$	$f_{t-1}-f_c$	Δf^e	f_t	are f	Rainfall Excess
0	0								2.000		
1	0.05	.450	2.35	-.05	.15	-.064	1.900	-.121	2.121	2.060	--
2	0.10	.375	2.40	0	.20	0	2.021	0	2.121	2.121	--
3	0.15	.429	2.45	.05	.25	.035	2.021	.071	2.050	2.086	--
4	0.30	.650	2.60	.20	.40	.125	1.950	.244	1.806	1.928	--
5	0.40	.994	2.70	.30	.50	.221	1.706	.377	1.429	1.618	--
6	0.50	1.471	2.80	.40	.60	.350	1.329	.465	0.964	1.196	--
7	0.70	2.136	3.00	.60	.80	.534	.864	.461	0.503	0.734	--
8	0.60	2.497	2.90	.50	.70	.615	.403	.248	0.255	0.379	.221
9	1.00	3.145	3.30	.90	1.10	.780	.155	.121	0.134	0.194	.806
10	0.05	2.316	2.35	-.05	.15	-.328	.034	-.011	0.145	0.140	--
11	0.04	2.295	2.34	-.06	.14	-.347	.045	-.016	0.161	0.153	--
12	0.03	2.265	2.33	-.07	.13	-.523	.061	-.032	0.193	0.177	--
13	0.02	2.227	2.32	-.08	.12	-.640	.093	-.060	0.253	0.233	--
14	0.02	2.167	2.32	-.08	.12	-.623	.153	-.095	0.348	0.300	--
Total	3.96										1.027

[a] $A = R_t + f_c - f_{t-1}$

[b] $B = R_t + f_a + f_c$

[c] $C = R_t - f_c$

[d] $D = R_t + f_c$

[e] $\Delta f = \left(\frac{A}{B}\right)\left(\frac{C}{D}\right)\left(f_{t-1} - f_c\right)\Delta t$

Figure 7 is a graphic representation of a different rainfall situation and different watershed characteristics. For this example two different starting values are shown which result in different volumes of rainfall excess. Systematic trial values of f_o are necessary until an intake curve is computed which provides rainfall excess just equal to the volume of total storm response.

Projection - The watershed intake function was developed for the Walker Branch Watershed Project. It was tested by computing many intake functions for differing values of f_o, f_a, and f_c. All computed curves were acceptable on the basis of general configuration and empirical evidence from other similar watersheds. It is necessary to estimate f_a and f_c for the Walker Branch Watersheds based on the extent of the various soils groups and their infiltration properties.

It is hypothetically possible to apply the intake Eq. 10 to subportions of the watersheds if rainfall and/or soil characteristics make gross watershed averages appear unrealistic. It is also possible that in some secondary system of analyses f_o, f_a, and f_c can be found by curve-fitting procedures which will relate and scale these properties to soil moisture, surface hydrologic condition, and soil characteristics on many research watersheds.

No method is presently known by which theoretical "point infiltration" functions can be integrated over complex watershed space and complex rainfall time to produce rigorous solutions for watershed intake.

Watershed Transfer Function

Up to this point the volumetric relationship between rainfall on the watersheds and consequential streamflow has been established for each

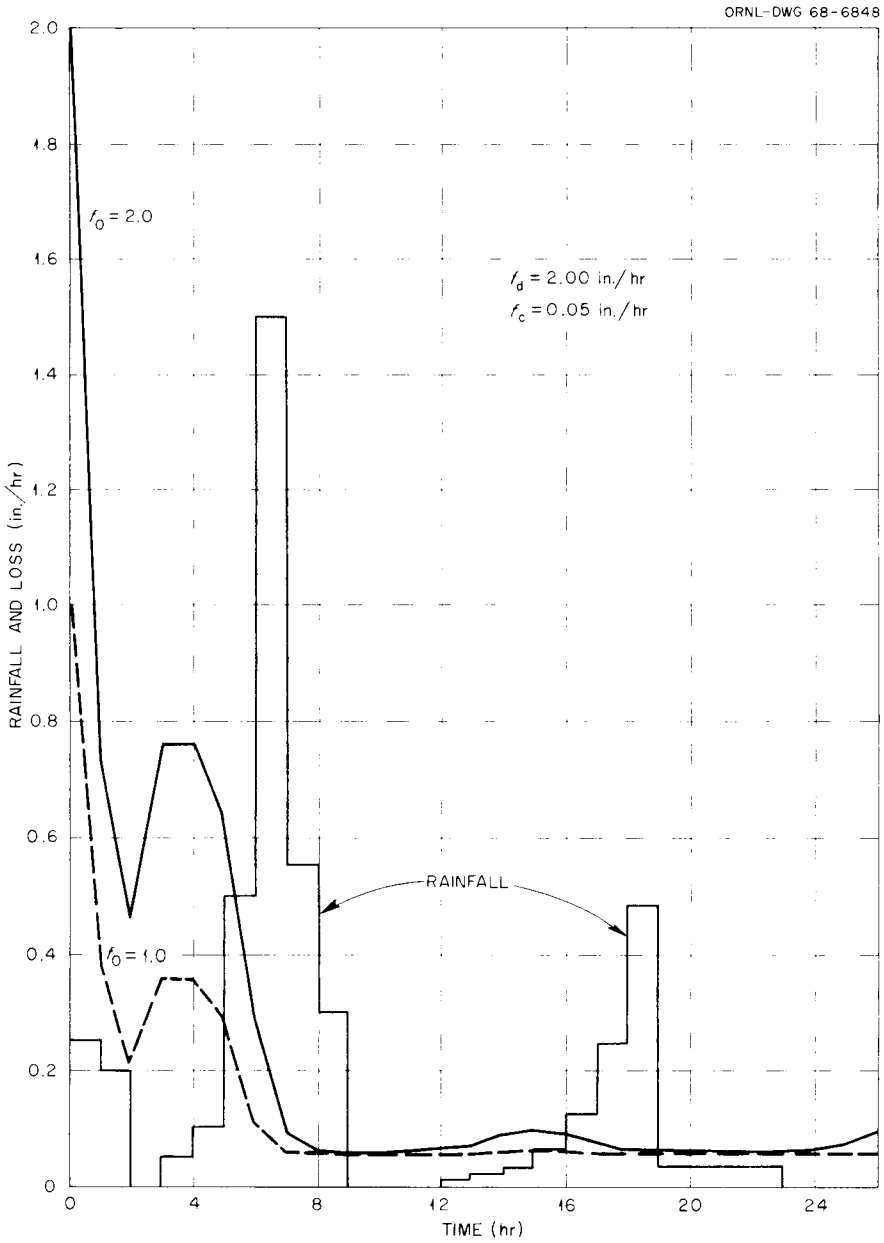

Fig. 7. Comparison of Rainfall Excess Determined for Two Different Starting Values, f_o = 2.0, and f_o = 1.0, holding f_d and f_e constant.

storm that occurs. The distribution of rainfall excess in sequential periods of time during the storm has also been established. There remains to develop some mathematical representation of the process by which rainfall is temporarily stored in the watershed and gradually released to form streamflow. Some lapse of time is required to physically pass the excess rainfall from its point of impact in the watershed to the point of concentration at the stream gage. During this passage rapid fluctuations in rainfall are filtered which results in smoother and more gradual fluctuations in streamflow than in original rainfall.

As in the case of the watershed intake function, no methods are presently known for rigorous determination of the process which will convert rainfall excess to streamflow. Instead, the systems analysis approach of correlating inflow and outflow must be followed. A functional form is hypothesized which will operate on the rainfall input to generate the streamflow output.

Inflow-Outflow Computation

Table 2 shows the computation of streamflow at discrete time units. For this example values of stream discharge, Q_t, are generated by operating on four sequential values of rainfall excess, $r(\tau)$, by a transfer function, $\mu(\tau)$. The entire process is a discrete form of the convolution integral (3) shown in Eq. 11.

$$Q_t = \int_0^t r(\tau)\ \mu\ (t-\tau)\ d\tau \tag{11}$$

where t is real time during the storm, and τ is a time parameter of integration. The discrete form is generally used in hydrologic practice because mathematical functions for $r\ (\tau)$ and $\mu\ (\tau)$ are not normally known.

Table 2. Form of Inflow - Outflow Computation

Units of Time	Ordinates of the Transfer Function	Discrete Convolution: Time Increments of Rainfall Excess (Inflow) r_1 r_2 r_3 r_4		Total Stream Response (Outflow)
1	u_1	r_1u_1	=	Q_1
2	u_2	$r_1u_2 + r_2u_1$	=	Q_2
3	u_3	$r_1u_3 + r_2u_2 + r_3u_1$	=	Q_3
4	u_4	$r_1u_4 + r_2u_3 + r_3u_2 + r_4u_1$	=	Q_4
5	u_5	$r_1u_5 + r_2u_4 + r_3u_3 + r_4u_8$	=	Q_5
6	u_6	$r_1u_6 + r_2u_5 + r_3u_4 + r_4u_3$	=	Q_6
7	u_7	$r_1u_7 + r_2u_6 + r_3u_5 + r_4u_4$	=	Q_7
---	---			
---	---			
---	---			
N-3	u_{N-3}			
N-2	u_{N-2}			
N-1	u_{N-1}			
N	u_N	$r_1u_N + r_2u_{N-1} + r_3u_{N-2} + r_4u_{N-3}$	=	Q_N

In the set of equations in Table 2 it can be seen that N simultaneous equations express N ordinates of the total stream response hydrograph. These N ordinates are known following the isolation of the current storm from the antecedent recession. The increments of rainfall excess are known following trial and error application of the loss equation. Therefore, only the set of ordinates, u_t, of the transfer function are unknown.

Since the number of unknowns and the number of equations are equal, the set of equations could be solved for the unknown ordinates. In fact, a triangular condition exists at the beginning of the storm so that such a solution is extremely easy. However, a different method of solution is required since many errors and indeterminant elements are present. Therefore, a method of solution is used which produces some average or optimum set of u_t's in the presence of such errors. Solution by the method of least squares can accomplish such an "averaging" solution.

In order for an averaging process to work it is necessary to reduce the number of unknowns to some order less than the number of equations. This reduction is possible by interpolating for some of the u_t's from adjacent values. Many types of interpolation are possible, from simple linear to polynomial or trigonometric forms. The linear forms lead to segmented functions, which are easy to use with non-uniformily spaced ordinates, and are the forms chosen for the Walker Branch Watershed analysis.

Form of the Transfer Function

The general procedure in hydrologic analysis has been to specify some functional form and then evaluate this transfer function by the input-output

correlation. Following the conventional approach, the same functional form is evaluated for each storm. Any optimizing, or fitting procedure, can only give the "best" shape parameters of that function. There is no direct evidence as to whether the form of the function is changing from storm to storm. A different procedure is both desirable and possible (4).

The approach used in this report is to consider the transfer function to be made up of a series of connected straight-line segments. Examples of such transfer functions are shown in Fig. 8. These segmented functions are approximations of smoothly-continuous but unknown functions. One must realize that the linear segments are not simply chords of the underlying smooth functions; rather, the segmented forms must be considered optimized substitutions for the continuous forms.

A full understanding of the concept of linear segmented forms as substitutions for smoothly continuous curvilinear forms can be gained from an example taken from (4). This example considers a 5-point set of values y_1, y_2, y_3, y_4, and y_5, assumed taken from some continuous function. It is desired to substitute two linear segments for this set. The first segment is specified by ordinates y_1' and y_3'. The second segment is specified by ordinates y_3' and y_5', the two segments thus have the value y_3' in common. If the values are uniformly spaced along a time axis, the value to substitute for y_2 is $(y_1' + y_3')/2$. Similarly the value to substitute for y_4 is $(y_3' + y_5')/2$. An error exists between each pair, which may be defined by $y_1 - y_1'$, $y_2 - (y_1' + y_3')/2$, and so on. An optimal substitution of the two segments for the original 5-point set is accomplished by least squares. While it has been specified that a hinge between the segments is located at the central value, no functional values are pre-set.

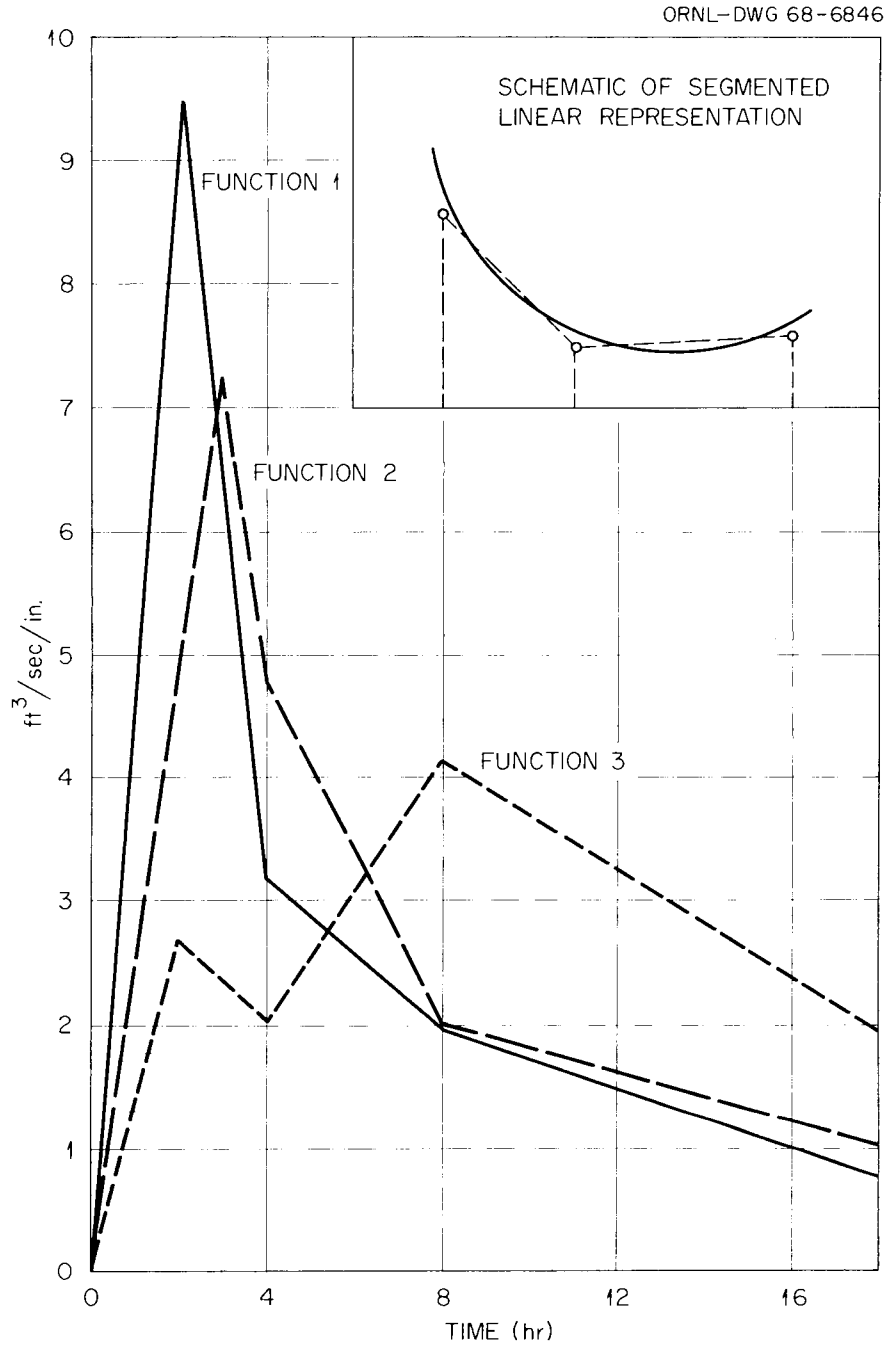

Fig. 8. Examples of Linear Segmented Transfer Functions Computed from Input-Output Correlations.

The use of least squares as the transformation process proceeds as follows. The algebraic expressions for the 5 errors are squared and totaled. The expression contains three unknowns; y_1', y_3' and y_5'. These unknowns may be considered variables since it is desirable to allow them to seek such values so that the sum of the 5 squared errors is a minimum. It is a simple process to partially differentiate the total squared error with respect to each of the three unknowns. This set of equations is set equal to zero for the condition of minimization and the equations are solved simultaneously. Values for y_1', y_3', y_5' result directly. Values for y_2' and y_4' are obtained by the simple linear interpolation specified by the segmented functional form.

The solution is presented in the set of Eqs. 12. This was the set of Eqs. 7 in the reference paper (4).

$$
\begin{aligned}
y_1' &= (1/35)(29y_1 + 12y_2 - 5y_3 - 2y_4 + y_5) \\
y_2' &= (1/70)(24y_1 + 22y_2 + 20y_3 + 8y_4 - 4y_5) \\
y_3' &= (1/7)(-y_1 + 2y_2 + 5y_3 + 2y_4 - y_5) \\
y_4' &= (1/70)(-4y_1 + 8y_2 + 20y_3 + 22y_4 + 24y_5) \\
y_5' &= (1/35)(y_1 - 2y_2 - 5y_3 + 12y_4 + 29y_5)
\end{aligned}
\tag{12}
$$

Following the solution for the segmented functional values the errors can be computed. These are the differences between the original points and the computed points. The 5 error-equations are presented in Eqs. 13. This was the set of Eqs. 8 in the reference paper (4).

$$
\begin{aligned}
E_1 &= (1/35)(6y_1 - 12y_2 + 5y_3 + 2y_4 - y_5) \\
E_2 &= (1/70)(-24y_1 + 48y_2 - 20y_3 - 8y_4 + 4y_5) \\
E_3 &= (1/7)(y_1 - 2y_2 + 2y_3 - 2y_4 + y_5) \\
E_4 &= (1/70)(y_1^4 - 8y_2 - 20y_3 + 48y_4 - 24y_5) \\
E_5 &= (1/35)(-y_1 + 2y_2 + 5y_3 - 12y_4 + 6y_5)
\end{aligned}
\tag{13}
$$

Equations 13 and their derivation now illustrate three primary points: 1) The errors at all points enter into the solution, including those values where interpolations are made. 2) While the location of the hinge must be specified, this does not determine the value of transformed points. Rather transformation by least squares establishes the values. 3) Only three values (unknowns) were determined. In the example a 5-to-3 averaging of the errors was thus obtained.

Analytical Transformation of the Transfer Function - The approximating form of the transfer function, illustrated by the straight-line segments of Fig. 8, will now be combined with the discrete convolution in Table 2. First, however, the algebraic form of the substitution will be given. This is expressed by the set of equations in Table 3. The transformation is accomplished by specifying ordinates at the angle-points where linear segments connect. At these points the ordinates plus some unknown error equal the ordinates of the original transfer function. The intermediate ordinates of the linear segments can be inserted directly by simple linear interpolation. These interpolated values plus some unknown error also equal the corresponding ordinates of the original transfer function.

The enforcement of an averaging process is evident in Table 3. The 20 unknown discrete ordinates of the original transfer function have been reduced to 8 unknown ordinates of the approximating linear segments. The ordinate O_{11}, for example, now occurs in 6 of the equations, and a method of solution, such as by least squares, must produce some best average value in these 6 equations. It should be specifically noted that the substitution of linear segments is not made by drawing chords across selected areas of the original function. All ordinates of the approximating

Table 3. Transformation of the Transfer Function

Units of Time	Ordinates of the Transfer Function		Approximating Linear Segments				Angle Points
1	u_1	=	$1/2\ O_2$	+		E_1	
2	u_2	=	O_2	+		E_2	*
3	u_3	=	$1/2\ (O_2 + O_4)$	+		E_3	
4	u_4	=	O_4	+		E_4	*
5	u_5	=	O_5	+		E_5	*
6	u_6	=	O_6	+		E_6	*
7	u_7	=	$1/2\ (O_6 + O_8)$	+		E_7	
8	u_8	=	O_8	+		E_8	*
9	u_9	=	$1/3(2O_8 + O_{11})$	+		E_9	
10	u_{10}	=	$1/3\ (O_8 + 2O_{11})$	+		E_{10}	
11	u_{11}	=	O_{11}	+		E_{11}	*
12	u_{12}	=	$1/4(3O_{11} + O_{15})$	+		E_{12}	
13	u_{13}	=	$1/4(2O_{11} + 2O_{15})$	+		E_{13}	
14	u_{14}	=	$1/4\ (O_{11} + 3O_{15})$	+		E_{14}	
15	u_{15}	=			O_{15} +	E_{15}	
16	u_{16}	=	$1/5(4O_{15} + O_{20})$	+		E_{16}	
17	u_{17}	=	$1/5(3O_{15} + 2O_{20})$	+		E_{17}	
18	u_{18}	=	$1/5(2O_{15} + 3O_{20})$	+		E_{18}	
19	u_{19}	=	$1/5\ (O_{15} + 4O_{20})$	+		E_{19}	
20	u_{20}	=	O_{20}	+		E_{20}	*

function, including those at angle points, will differ from the original function. In fact, the placement of the approximating function over the original function can only be accomplished by specifying some optimization process operating on the ordinate errors, E.

If a transfer function $u_t(t = 1, 20)$ were known, the set of equations in Table 3 could be solved directly by least squares to get an optimum set of linear ordinates, the O's. However, in practical storm analysis the u_t's are not known, and the set of ordinates, O, must be derived directly from the storm rainfall and streamflow.

Solution for the Linear-Segmented Hydrograph - The transforming equations of Table 3 may be substituted into the discrete convolution of Table 2. The result is a system of linear equations relating rainfall excess, the transformed transfer function, and the total stream response hydrograph. This set of equations is shown in Table 4. In Table 4 the ordinate errors shown in Table 3 have not been given explicitly. In order to produce an "averaged" solution of the Table 4 equations some residual error must also be considered attached to each equation of the set. The transform errors of Table 3 are thus combined with the discrete convolution errors in Table 4.

It is possible to rearrange the left-hand sides of the Table 4 equations. An arrangement by collection of terms with common ordinates is shown in Table 5. The common ordinates are factored out and placed at the head of the respective columns. The equal signs and the plus signs between major segments of the equations have also been omitted.

Table 5 provides an arrangement of data, the rainfall excess terms, and stream hydrograph ordinates, which permits direct application of the

Table 4. Convolution with Transformed Function

Units of Time	r_1		r_2		r_3		r_4		Total Stream Response
1	$1/2\ r_1\ O_2$							=	Q_1
2	$r_1\ O_2$	+	$1/2\ r_2 O_2$					=	Q_2
3	$1/2\ r_1\ (O_2 + O_4)$	+	$r_2 O_2$	+	$r_3 O_2$			=	Q_3
4	$r_1\ O_4$	+	$1/2\ r_2\ (O_2 + O_4)$	+	$r_3 O_2$	+	$1/2\ r_4 O_2$	=	Q_4
5	$r_1\ O_5$	+	$r_2 O_4$	+	$1/2\ r_3\ (O_2 + O_4)$	+	$r_4 O_2$	=	Q_5
6	$r_1\ O_6$	+	$r_2 O_5$	+	$r_3 O_4$	+	$1/2\ r_4\ (O_2 + O_4)$	=	Q_6
7	$1/2\ r_1\ (O_6 + O_8)$	+	$r_2 O_6$	+	$r_3 O_5$	+	$r_4 O_4$	=	Q_7
8	$r_1\ O_8$	+	$1/2\ r_2\ (O_6 + O_8)$	+	$r_3 O_6$	+	$r_4 O_5$	=	Q_8
9	$1/3\ r_1\ (2O_8 + O_{11})$	+	$r_2 O_8$	+	$1/2\ r_3\ (O_6 + O_8)$	+	$r_4 O_6$	=	Q_9
10	$1/3\ r_1\ (O_8 + 2O_{11})$	+	$1/3\ r_2 (2O_8 + O_{11})$	+	$r_3 O_8$	+	$1/2\ r_4\ (O_6 + O_8)$	=	Q_{10}
11	$r_1\ O_{11}$	+	$1/3\ r_2\ (O_8 + 2O_{11})$	+	$1/3\ r_3 (2O_8 + O_{11})$	+	$r_4 O_8$	=	Q_{11}

Table 5. Arrangement for Least-squares Solution of Transfer Function

Time	Transfer Function Ordinates								Total Stream Response
	O_2	O_4	O_5	O_6	O_8	O_{11}	O_{15}	O_{20}	
1	$\frac{1}{2}r_1$								Q_1
2	$r_1 + \frac{1}{2}r_2$								Q_2
3	$\frac{1}{2}r_1 + r_2 + \frac{1}{2}r_3$	$\frac{1}{2}r_1$							Q_3
4	$\frac{1}{2}r_2 + r_3 + \frac{1}{2}r_4$	$r_1 + \frac{1}{2}r_2$							Q_4
5	$\frac{1}{2}r_3 + r_4$	$r_2 + \frac{1}{2}r_3$	r_1						Q_5
6	$\frac{1}{2}r_4$	$r_3 + \frac{1}{2}r_4$	r_2	r_1					Q_6
7		r_4	r_3	$\frac{1}{2}r_1 + r_2$	$\frac{1}{2}r_1$				Q_7
8			r_4	$\frac{1}{2}r_2 + r_3$	$r_1 + \frac{1}{2}r_2$				Q_8
9				$\frac{1}{2}r_3 + r_4$	$\frac{2}{3}r_1 + r_2 + \frac{1}{2}r_3$	$\frac{1}{3}r_1$			Q_9
10				$\frac{1}{2}r_4$	$\frac{1}{3}r_1 + \frac{2}{3}r_2 + r_3 + \frac{1}{2}r_4$	$\frac{2}{3}r_1 + \frac{1}{3}r_2$			Q_{10}
11					$\frac{1}{3}r_2 + \frac{2}{3}r_3 + r_4$	$r_1 + \frac{2}{3}r_2 + \frac{1}{3}r_3$			Q_{11}
12					$\frac{1}{3}r_3 + \frac{2}{3}r_4$	$\frac{3}{4}r_1 + r_2 + \frac{2}{3}r_3 + \frac{1}{3}r_4$	$\frac{1}{4}r_1$		Q_{12}
13					$\frac{1}{3}r_4$	$\frac{2}{4}r_1 + \frac{3}{4}r_2 + r_3 + \frac{2}{3}r_4$	$\frac{2}{4}r_1 + \frac{1}{4}r_2$		Q_{13}
14						$\frac{1}{4}r_1 + \frac{2}{4}r_2 + \frac{3}{4}r_3 + r_4$	$\frac{3}{4}r_1 + \frac{2}{4}r_2 + \frac{1}{4}r_3$		Q_{14}
15						$\frac{1}{4}r_2 + \frac{2}{4}r_3 + \frac{3}{4}r_4$	$r_1 + \frac{3}{4}r_2 + \frac{2}{4}r_3 + \frac{1}{4}r_4$		Q_{15}
16						$\frac{1}{4}r_3 + \frac{2}{4}r_4$	$\frac{4}{5}r_1 + r_2 + \frac{3}{4}r_3 + \frac{2}{4}r_4$	$\frac{1}{5}r_1$	Q_{16}
17						$\frac{1}{4}r_4$	$\frac{3}{5}r_1 + \frac{4}{5}r_2 + r_3 + \frac{1}{4}r_4$	$\frac{2}{5}r_1 + \frac{1}{5}r_2$	Q_{17}
18							$\frac{2}{5}r_1 + \frac{3}{5}r_2 + \frac{4}{5}r_3 + r_4$	$\frac{3}{5}r_1 + \frac{2}{5}r_2 + \frac{1}{5}r_3$	Q_{18}
19							$\frac{1}{5}r_1 + \frac{2}{5}r_2 + \frac{3}{5}r_3 + \frac{4}{5}r_4$	$\frac{4}{5}r_1 + \frac{3}{5}r_2 + \frac{2}{5}r_3 + \frac{1}{5}r_4$	Q_{19}
20							$\frac{1}{5}r_2 + \frac{2}{5}r_3 + \frac{3}{5}r_4$	$r_1 + \frac{4}{5}r_2 + \frac{3}{5}r_3 + \frac{2}{5}r_4$	Q_{20}

method of least squares for solution of the set of transfer function ordinates, O. The values of 8 ordinates will be averaged over 20 stream ordinates by least-square definition. It can be seen that the system of interpolation for the linear-segmented transfer function has produced a set of numeric operators on the rainfall excess terms. Such operations on the excess terms produce the X's of a multiple regression equation. The storm hydrograph ordinates, Q, are obviously the Y's of a multiple regression.

The example shown here is for a matrix dimension produced by 20 storm ordinates and 4 periods of rainfall excess. However, the basic concepts are general. Any number of storm ordinates could be used with any number of rainfall terms. Other transforms of the transfer function than that shown in Table 3 could also be used. The entire process is being programmed for electronic data processing for application to all storms of record on Walker Branch Watershed. Following such application for solution of the "angle-point" ordinates specified in Table 5, the ordinates between angle points can be found by the linear interpolation indicated under "Approximating Linear Segments" in Table 3.

The concept of a segmented transfer function produces a linearized and discrete convolution form. This simplified form does not require much time or effort, either in preliminary data arrangement or in storm analysis, when considering systematic processing of all storms in a hydrologic record.

Time-Separated Hydrographs

The Re-constructed Hydrograph - It is well known that stream response to a storm can be computed from the increments of rainfall excess and the ordinates of a transfer function, as shown by the discrete convolution in

Table 2. In earlier analytical techniques the transfer function was usually determined from only a small number of selected storms meeting idealized criteria. Its suitability for use with long-duration storms of complex rainfall pattern was determined by trial computation. The computed ordinates were compared, usually graphically, with the observed storm ordinates.

After a linear segmented transfer function has been determined by least squares, it can also be applied to the increments of rainfall excess, and the total stream response can be calculated. This process is identical to the computation of "predicted values" for comparison with "observed values" in ordinary multiple regression analysis. The "predicted values" form a reconstructed version of the stream response. It should be noted that the total response above the antecedent base flow is reconstructed.

Partially Re-constructed Hydrographs - Normally it is not recognized that partial values of the reconstructed storm hydrograph can be used to form a time-separated hydrograph. This procedure will be developed by considering the full set of transfer function ordinates, O, which are approximations for the u's in Table 2.

The area enclosed by the polygon defined by the ordinates O represents unit volume of total runoff. Even though continuity of mass was not specifically stated, it is implicit in the equations in Table 2. If the time-base of the transfer function is N time units long, then all the ordinates from time zero to time N define the total volumetric distribution. However, if one considered dropping the ordinate O_N, then the partial transfer function, defined by ordinates from time zero to time N-1 must represent a reduced volume. The volume unaccounted for is the

volume of water with travel-time through the watershed ranging from N-1 to N. The same logic applies to any ordinate at some time T between zero and N. The partial transfer function composed of ordinates from zero to T represents the volume of water with travel time < T.

One can now consider the effect of systematic elimination of the terms from the equations in Table 2. If one drops the terms in the left sides of these equations which contain O_1 (substituted for u_1), then the first four stream response ordinates are reduced. This reduction represents water with travel time from zero to one time unit. If now the O_2 terms are additionally dropped, this further reduction represents volume of water with travel time from one to two time units. Systematic dropping of the transfer function terms produces sets of partial response ordinates. By plotting all such sets of partial ordinates under the storm hydrograph, a time-separated hydrograph is produced.

Examples of Time Separated Hydrographs - Figure 9 shows a time separated hydrograph constructed from the Transfer Function 1 of Fig. 8 and the increments of rainfall excess as shown. Figure 10 shows a time separated hydrograph constructed from the same rainfall excess but using Transfer Function 2 from Fig. 8.

In Figs. 9 and 10 the solid bounding line represents total stream response to the input rainfall excess. As such it represents increase in streamflow above antecedent flow regardless of whether this increase is called surface, subsurface, or ground-water runoff. The time separation lines were constructed for delay time increments of one hour. Areas on the graph between indicated delay times represent volumes of flow between these delay times.

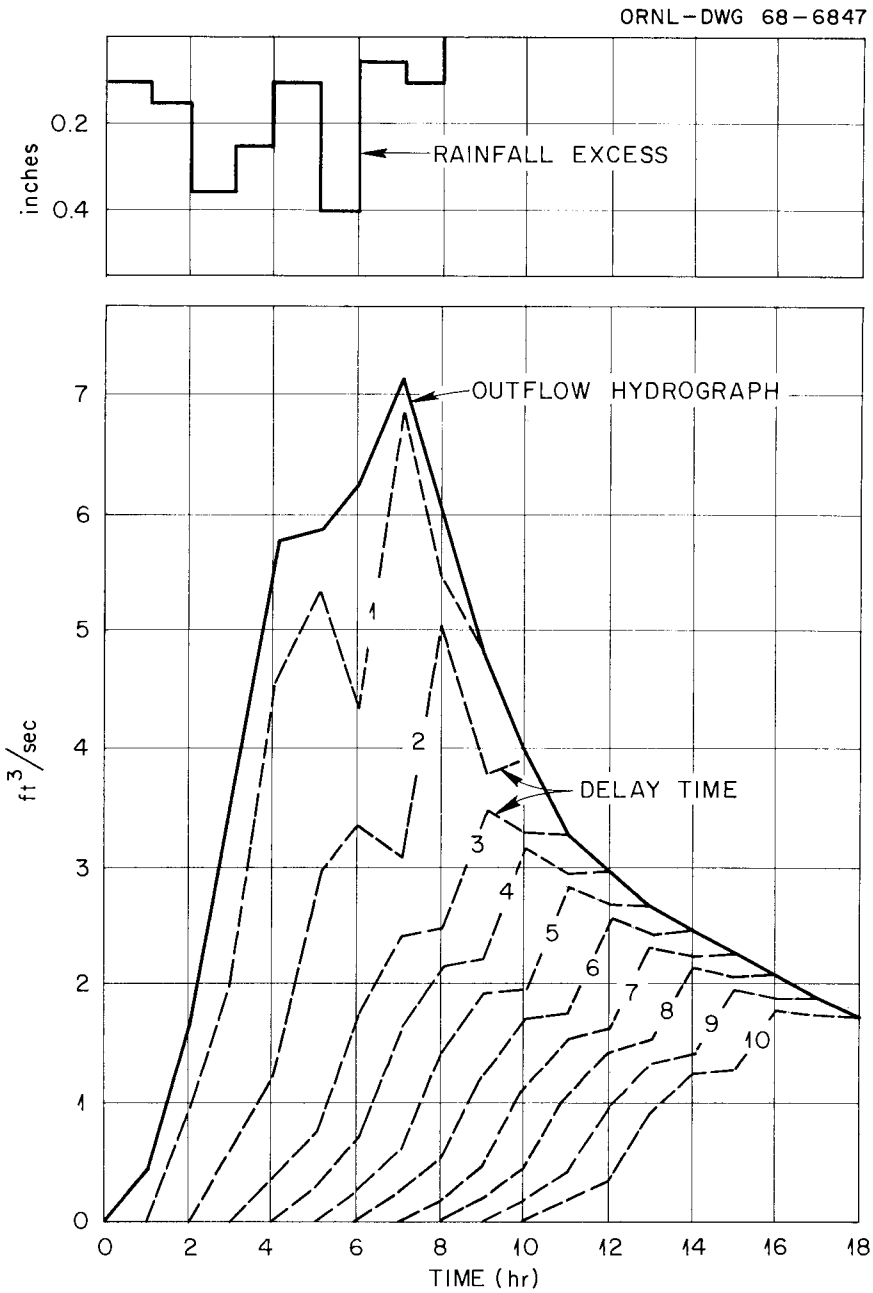

Fig. 9. A Time Separated Hydrograph Constructed from Transfer Function 1 of Fig. 8, p. 37.

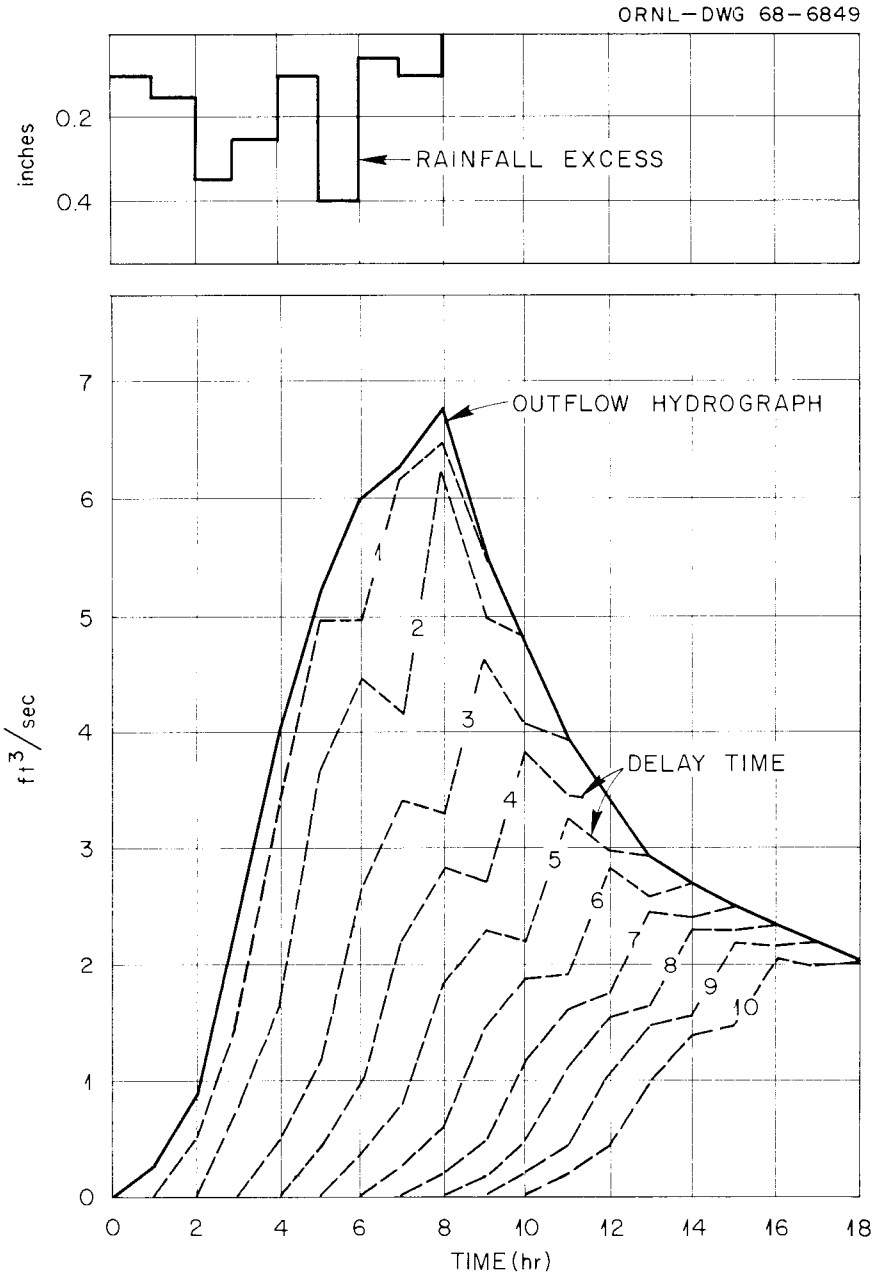

Fig. 10. A Time Separated Hydrograph Constructed from the Same Rainfall Excess in Fig. 9, p. 47, but Using Transfer Function 2 of Fig. 8, p. 37.

Figure 9 shows a total peak slightly higher than that of Fig. 10 because of the higher peak ordinate of the associated transfer function. A more striking difference, however, is found in the volumes of water with short delay times. Figure 9 contains a much greater volume in 0- to 3-hour delay time than does Fig. 10. Beyond about 3 hours delay time the pattern of separation is similar in the two figures, though delayed flows are somewhat greater in Fig. 10.

The more rapid response of the watershed implied in Transfer Function 1 as compared to Transfer Function 2 can be effectively demonstrated by comparing the ordinates at 4 hours in Figs. 9 and 10. The total ordinate is about 5.8 cfs in Fig. 9. The portion of the ordinate with delay time of zero to two hours is 4.5 cfs. In Fig. 10, on the other hand, the total ordinate is 4 cfs. But the portion of this ordinate with delay time of zero to two hours is only 2.3 cfs.

Now consider some sample for chemical analysis taken at time 4 hours in Figs. 9 and 10. Consider further that presence of this chemical in the stream is associated with a surface source area, and, therefore, with surface-derived runoff. It would be expected that a higher absolute value of the chemical would be found with the 4.5 cfs rapid response of Fig. 9 than with the 2.3 cfs rapid response of Fig. 10. Similar differences can be inferred at other times in the outflow hydrographs.

Specific Transfer Functions for Walker Branch Watersheds

The principles of linearized watershed transfer functions, and their use in reconstruction of storm hydrographs have been discussed. Specific forms for the Walker Branch Watershed are discussed below.

An important feature of the program is that the hydrograph of each storm will be analyzed separately. It is anticipated that rainfall amounts and durations will vary greatly, from abrupt, intensive, summer thunderstorm types, to prolonged, moderate, winter cyclonic types. Short storms require information at close intervals to produce a precise description of rainfall and streamflow fluctuations. Prolonged storms do not require information at close intervals and use of the original data punched at 5-minute intervals would be inefficient computer usage. Consequently a varying base period for the interval between data points was chosen, the periods being integral numbers of 5-minute periods. Long duration storms can thus be treated with rainfall composited from several 5-minute periods. Streamflow data are also spaced at these longer intervals.

Storm Scales - An expanding system of time scales was designed to cover a great range of storm duration. Table 6 shows the scales with pertinent storm characteristics. The scales are determined by an expansion factor of 4. Scale a is used with short-duration storms, uses rainfall input in 5-minute increments and analyzes a 6-hour segment of the resulting stream hydrograph. Scale d is applied to long storms, uses rainfall input in 320-minute increments and analyzes a 16-day segment of the stream hydrograph. Scales b and c are for storms of intermediate duration.

After rainfall amounts and durations are determined for each storm occurrence, as described in the section "Definition and Detection of Storms," p. 6, the appropriate scale for storm analysis is chosen. The scale is set by comparing storm duration with "Upper Limit of Rainfall Duration" in Table 6.

Table 6. Time Scales for Hydrograph Analysis

Scale	Input Unit of Rainfall (min)	Upper Limit of Rainfall Duration (5-min Periods)	(hrs)	Base of Transfer Function (hrs)	(days)
a	5	12	1	6	1/4
b	20	48	4	24	1
c	80	192	16	96	4
d	320	768	64	384	16

Linearization of Transfer Function - In earlier discussion of the linearly segmented transfer function it was pointed out that the positions of the connections, or "hinges" between the segments must be arbitrarily selected. Table 7 shows the position of the hinges chosen for the transfer function for the Walker Branch Watershed project. The scales in this table are identical to those in Table 6.

Data Manipulation - Following determination of the appropriate scale-factor for a storm it is necessary to arrange both stored rainfall and streamflow data into suitable form for least-squares determination of the numerical values of the transfer function ordinates.

Rainfall is arranged by accumulating 5-minute increments into "scale-period" increments. For example, for Scale b storm rainfall is incremented by 20-minute periods. No change is necessary for Scale a storms since these use 5-minute units of rainfall.

Streamflow ordinates must also be determined at "scale-period" intervals. Again, using Scale b as an example, ordinates must be determined at 20-minute intervals. Since the streamflow data are not "stored" at required intervals, the necessary values must be determined by interpolation. Simple linear interpolation is sufficient since data points selected for storage would include all those needed to describe the storm hydrograph.

Consider streamflow data points stored in the form Q (I) and t (I) where Q is discharge, t is time, and I is an index describing relative position in time sequence. Compute a time parameter, $t' = (SU)(J)$, in which SU is the scale unit of time (same as "Input Unit of Rainfall" in Table 6) and J is the sequence of "Basic Time Units" in Table 7. Then

Table 7. Linearized Transfer Function Walker Branch Watershed

Basic Time Units (a, b, c, or d Scales)	Transfer Function (cfs)	Hinge Locations	Time for Scale a (mins)	b (hrs)	c (hrs)	d (hrs)
0	zero					
1	0	*	5	1/3	1-1/3	5-1/3
2	$1/2(0_1 + 0_3)$					
3	0	*	15	1	4	16
4	$1/3(20_3 + 0_6)$					
5	$1/3(0_3 + 20_6)$					
6	0_6	*	30	2	8	32
7	$1/4(30_6 + 0_{10})$					
8	$1/4(20_6 + 20_{10})$					
9	$1/4(0_6 + 30_{10})$					
10	0_{10}	*	50	3-1/3	13-1/3	53-1/3
11	$1/8(70_{10} + 0_{18})$					
12						
13						
14						
15						
16						
17	$1/8(0_{10} + 70_{18})$					
18	0_{18}	*	90	6	24	96
19	$1/12(110_{18} + 0_{30})$					
****	***					
29	$1/12(0_{18} + 110_{30})$					
30	0_{30}	*	150	10	40	160
31	$1/18(170_{30} + 0_{48})$					
****	***					
47	$1/18(0_{30} + 170_{48})$					
48	0_{48}	*	240	16	64	256
49	$1/24(230_{48} + 0_{72})$					
****	***					
71	$1/24(0_{48} + 230_{72})$					
72	0_{72}		360	24	96	384
73	$1/24(-0_{48} + 250_{72})$					
74	$1/24(-20_{48} + 260_{72})$					
****	***					
84	$1/24(-120_{48} + 360_{72})$					

t' can be located in the record by the criterion $t[I] < t' \leqq t[I+1]$. Following this an interpolated ordinate for each value J can be computed by Eq. 14.

$$Q(J) = \frac{t' - t[I]}{t[I+1]-t[I]} \times Q[I+1] - Q[I] + Q[I] \qquad (14)$$

All data are now ready for construction and solution of equations similar to Table 5, but are adapted specifically for Walker Branch Watershed.

REFERENCES

1. Curlin, J. W., and D. J. Nelson, Walker Branch Watershed Project: Objectives, facilities, and ecological characteristics. ORNL-TM-2271, 1968.

2. Johnson, E. A., and R. E. Dils, "Outline for compiling precipitation, runoff, and ground-water data from small watersheds." Southeastern Forest Experiment Station Paper 68, Asheville, North Carolina.

3. Spiegel, M. R., Laplace Transforms. Schaum Publishing Co., New York 1965.

4. Snyder, W. M. "Some Error Properties of Segmented Hydrologic Functions," Water Resources Research, Vol. 3, No. 2, 1967.

5. Jahnke, E. and F. Emde. Tables of Functions. Dover Publications, New York 1945, p. 20.

ORNL-4392
UC-41 — Health and Safety

INTERNAL DISTRIBUTION

1. Biology Library
2-4. Central Research Library
5. Laboratory Shift Supervisor
6-7. ORNL — Y-12 Technical Library Document Reference Section
8-41. Laboratory Records Department
42. Laboratory Records, ORNL R.C.
43. H. H. Abee
44. C. H. Abner
45-144. S. I. Auerbach
145. J. A. Auxier
146. C. G. Bell
147. B. G. Blaylock
148. M. Bender
149. W. T. Berg
150. S. R. Bernard
151. W. P. Bonner
152. W. J. Boegley, Jr.
153. C. J. Borkowski
154. G. E. Boyd
155. A. A. Brooks
156. F. R. Bruce
157. T. J. Burnett
158. C. C. Burwell
159. S. F. Carson
160. K. E. Cowser
161. J. S. Cromwell
162. F. L. Culler, Jr.
163-262. J. W. Curlin
263. R. C. Dahlman
264. W. DeLaguna
265. P. B. Dunaway
266. B. R. Fish
267. R. C. Fox
268. C. Francis
269. D. A. Gardiner
270. D. F. Grigal
271. T. Grizzard
272. R. P. Hammond
273. C. S. Harrill
274. F. F. Haywood
275. D. G. Jacobs
276. W. Johnston
277. S. V. Kaye
278. M. A. Kastenbaum
279. R. F. Kimball
280. J. T. Kitchings III
281. C. E. Larson
282. C. S. Lisser
283. J. L. Liverman
284. T. F. Lomenick
285. H. G. MacPherson
286. W. C. McClain
287. J. W. Michel
288. C. D. Miller
289. F. L. Miller
290. W. R. Miller
291. K. Z. Morgan
292-390. D. J. Nelson
391. D. R. Nelson
392. J. S. Olson
393. R. V. O'Neill
394. F. S. Patton
395. H. R. Payne
396. D. E. Reichle
397. A. F. Shinn
398. W. H. Sides, Jr.
399. M. J. Skinner
400. M. W. Snyder
401. W. S. Snyder
402. G. Stanhill
403. E. G. Struxness
404. C. E. Styron, Jr.
405. D. A. Sundberg
406. T. Tamura
407. F. G. Taylor, Jr.
408. D. G. Thomas
409. W. A. Thomas
410. V. R. R. Uppuluri
411. P. R. Vanstrum
412. F. C. Von der Lage
413. A. M. Weinberg
414. Robert Wichner
415. J. P. Witherspoon
416. M. Witkamp
417. Gale Young
418. J. E. Cantlon (consultant)
419. J. C. Frye (consultant)
420. E. Gerjuoy (consultant)
421. J. B. Hursh (consultant)
422. H. O. Wyckoff (consultant)

EXTERNAL DISTRIBUTION

423. J. N. Wolfe, Environmental Sciences Branch, Division of Biology and Medicine, USAEC, Washington, D. C. 20545
424. J. J. Davis, Environmental Sciences Branch, Division of Biology and Medicine, USAEC, Washington, D. C. 20545
425. R. F. Reitemeier, Environmental Sciences Branch, Division of Biology and Medicine, USAEC, Washington, D. C. 20545
426. W. S. Osburn, Environmental Sciences Branch, Division of Biology and Medicine, USAEC, Washington, D. C. 20545
427. C. L. Osterberg, Environmental Sciences Branch, Division of Biology and Medicine, USAEC, Washington, D. C. 20545
428. Jeff Swinebroad, Environmental Sciences Branch, Division of Biology and Medicine, USAEC, Washington, D. C. 20545
429. C. S. Shoup, Biology Branch, Oak Ridge Operations, USAEC, Oak Ridge, Tennessee 37830
430. Paul Krueger, Dept. of Civil Engineering, School of Engineering, Stanford University, Stanford, California 94305
431. D. W. Goodall, Ecology Center, College of Natural Resources, Utah State University, Logan, Utah 84321
432. S. P. Gessel, School of Forestry, University of Washington, Seattle, Washington 98105
433. Frank Pitelka, Museum of Vertebrate Zoology, University of California, Berkeley, California
434. J. A. C. Fortescue, Dept. of Fisheries and Forestry, Petawawa Forest Experiment Station, Chalk River, Ontario, Canada
435. R. H. Ellis, Vice President, Travelers Research Corp., 250 Constitution Plaza, Hartford, Connecticut 06103
436. Harve Carlson, Director, Division of Biological and Medical Research, National Science Foundation, Washington, D. C.
437. LaMont C. Cole, Langmuir Laboratory, Cornell University, Ithaca, New York 14850
438. R. H. Whittaker, Dept. of Population Biology, University of California, Irvine, California
439. Charles Cooper, Dept. of Conservation, School of Natural Resources, University of Michigan, Ann Arbor, Michigan 48104
440. David Gates, Missouri Botanical Gardens, St. Louis, Missouri 63110
441. George Hoffman, Missouri Botanical Gardens, St. Louis, Missouri 63110
442. N. S. Hall, Agricultural Laboratory, University of Tennessee, AEC, Oak Ridge, Tennessee
443. Clive Edwards, Ecology Institute, University of Tennessee, Knoxville, Tennessee 37916
444. C. H. Shelton, Dept. of Agricultural Engineering, University of Tennessee, Knoxville, Tennessee 37916
445. H. A. Fribourg, Dept. of Agronomy, University of Tennessee, Knoxville, Tennessee 37916
446. L. F. Seatz, Dept. of Agronomy, University of Tennessee, Knoxville, Tennessee 37816
447. J. D. Hewlett, School of Forestry, University of Georgia, Athens, Georgia 30601
448-497. W. M. Snyder, School of Civil Engineering, Georgia Institute of Technology, Atlanta, Georgia

498. Frederick Knight, Dept. of Forestry, School of Natural Resources, University of Michigan, Ann Arbor, Michigan 48104
499. Helmut Leith, Dept. of Botany, University of North Carolina, Chapel Hill, North Carolina 27514
500. L. B. Leopold, U.S. Geological Survey, Washington, D. C. 20242
501. Nicholas Clesceri, Bio-Environmental Engineering Division, Renssalaer Polytechnic Institute, Troy, New York 12181
502. Gene E. Likens, Dept. of Biological Science, Dartmouth College, Hanover, New Hampshire 03755
503. Orie Loucks, Dept. of Botany, University of Wisconsin, Madison, Wisconsin 53706
504. H. A. I. Madgwick, Dept. of Forestry and Wildlife, Virginia Polytechnic Institute, Balcksburg, Virginia 24061
505. John T. McGinnis, Assist. Prof. of Botany, University of Georgia, Athens, Georgia 30601
506. Robert McIntosh, Dept. of Biology, University of Notre Dame, South Bend, Indiana 46556
507. Louis Metz, Southeastern Forest Experiment Station, Research Triangle, Durham-Raleigh, North Carolina
508-509. Philip L. Johnson, Division of Biology and Medicine, National Science Foundation, 1800 G Street, N.W., Washington, D. C. 26550
510. F. G. Goff, School of Forestry, University of Missouri, Columbia, Missouri 65201
511. Jerry Kline, Argonne National Laboratory, Argonne, Illinois 60439
512. G. M. Van Dyne, Natural Resources Ecology Laboratory, Colorado State University, Fort Collins, Colorado 80521
513. Carl D. Monk, Dept. of Botany, University of Georgia, Athens, Georgia
514. E. P. Odum, Dept. of Zoology, University of Georgia, Athens, Georgia
515. F. C. Evans, Dept. of Zoology, University of Michigan, Ann Arbor, Michigan 48104
516. David G. Frey, Dept. of Zoology, Indiana University, Bloomington, Indiana 47401
517. Robert H. Giles, Jr., Dept. of Forestry and Wildlife, Virginia Polytechnic Institute, Blacksburg, Virginia 24061
518. Frank B. Golley, Institute of Ecology, University of Georgia, Athens, Georgia 30601
519. Steve Stephenson, Dept. of Botany and Plant Pathology, Michigan State University, East Lansing, Michigan 48823
520. Karl F. Wenger, Branch Chief for Silviculture, Division of Timber Management Res., USDA, Forest Service, Washington, D. C. 20250
521. John Wilkinson, Rensselaer Polytechnic Institute, Statistics and Operations Research, Troy, New York 12181
522. Robert Ball, Dept. of Fisheries, Michigan State University, East Lansing, Michigan 48823
523. Robert J. Beyers, Savannah River Ecology Laboratory, University of Georgia, Athens, Georgia 30601
524. Byron O. Blair, Agronomy Dept., Life Sciences Building, Purdue University, West Lafayette, Indiana 47907
525. F. H. Bormann, School of Forestry, Yale University, New Haven, Connecticut 06511
526. Murray F. Buell, Dept. of Botany, Rutgers University, New Brunswick, New Jersey 08900

527. John Cantlon, Dept. of Botany, Michigan State University, East Lansing, Michigan 48823
528. E. E. C. Clebsch, Dept. of Botany, University of Tennessee, Knoxville, Tennessee 37916
529. Richard G. Clements, Research Associate, Institute of Ecology, University of Georgia, Athens, Georgia 30601
530. William Cooper, Dept. of Zoology, Michigan State University, East Lansing, Michigan 48823
531. Grant Cottam, Dept. of Botany, University of Wisconsin, Madison, Wisconsin 53706
532. D. A. Crossley, Dept. of Entomology, University of Georgia, Athens, Georgia 30601
533. Troy C. Dorris, Aquatic Biology Laboratory, Oklahoma State University, Stillwater, Oklahoma 74074
534. Robert B. Platt, Dept. of Biology, Emory University, Atlanta, Georgia 30322
535. William Reiners, Dept. of Biological Sciences, Dartmouth College, Hanover, New Hampshire 03755
536. Peter J. Rennie, Canadian Dept. of Forestry, Petawawa Forest Experiment Station, Chalk River, Ontario, Canada
537. J. R. Wallis, IBM Corp., Watson Research Center, Yorktown Heights, New York 10598
538. Eliot C. Williams, Jr., Dept. of Biology, Wabash College, Crawfordsville, Indiana 47933
539. George M. Woodwell, Dept. of Biology, Brookhaven National Laboratory, Upton, New York 11973
540. Frank F. Hooper, School of Natural Resources, University of Michigan, Ann Arbor, Michigan 48104
541. G. W. Saunders, Dept. of Zoology, University of Michigan, Ann Arbor, Michigan 48104
542. Robert Zahner, Dept. of Forestry, University of Michigan, Ann Arbor, Michigan 48104
543. John W. Barrett, Head, Dept. of Forestry, University of Tennessee, Knoxville, Tennessee 37916
544. Paul Y. Burns, Director, School of Forestry and Wildlife Management, Baton Rouge, Louisiana 70803
545. George M. Jemison, Deputy Chief, U.S. Forest Service, Washington, D. C. 20250
546. John L. Gray, Dean, School of Forestry, University of Florida, Gainesville, Florida 32601
547. Leonard Leyton, Section Leader I.U.F.R.O. Commonwealth Forestry Institute, University of Oxford, South Parks Road, Oxford, England
548. Robert E. Dils, College of Forestry and Natural Resources, Colorado State University, Fort Collins, Colorado 80521
549. William D. Striffler, College of Forestry and Natural Resources, Colorado State University, Fort Collins, Colorado 80521
550. David M. Moehring, Dept. of Forestry and Range Management, Texas A and M University, College Station, Texas 77843
551. Thomas C. Nelson, Director, Southern Forest Experiment Station, U.S. Forest Service, New Orleans, Louisiana 70113

552. Richard D. Lane, Director, Northeastern Forest Experiment Station, U.S. Forest Service, Upper Darby, Pennsylvania
553. M. H. Drinkwater, Canada Dept. of Forestry, Calgary, Alberta, Canada
554. James E. Douglass, Coweeta Hydrologic Laboratory, U.S. Forest Service, Dillard, Georgia 30537
555. W. R. Boggess, Dept. of Forestry, University of Illinois, Urbana, Illinois 61801
556. Donald P. Duncan, School of Forestry, University of Missouri, Columbia, Missouri 65201
557. T. Ewald Maki, Dept. of Forest Management, School of Forestry, North Carolina State University, Raleigh, North Carolina 27607
558. V. L. Harper, School of Forestry, University of Florida, 305 Rolfs Hall, Gainesville, Florida
559. H. C. Storey, Division of Watershed, Recreation and Range Research, U.S. Forest Service, Washington, D. C. 20250
560. W. M. Zillgitt, Director, Southeastern Forest Experiment Station, Asheville, North Carolina
561. William C. Bramble, Dept. of Forestry and Conservation, Purdue University, Lafayette, Indiana 47907
562. E. L. Stone, Jr., Dept. of Agronomy, Cornell University, Ithaca, New York 14850
563. Kenneth D. Carlander, Dept. of Zoology and Entomology, Iowa State University, Ames, Iowa 50010
564. Robert S. Campbell, Dept. of Zoology, University of Missouri, Columbia, Missouri 65201
565. Keith V. Slack, U.S. Geological Survey, 345 Middlefield Road, Menlo Park, California 94025
566. George Sprugel, Jr., Illinois Natural History Survey, Urbana, Illinois 61801
567. R. H. Moneymaker, Soil Conservation Service, U.S. Dept. of Agriculture, Knoxville, Tennessee
568. C. H. Stoltenberg, School of Forestry, Oregon State University, Corvallis, Oregon 97330
569. K. R. Knoerr, School of Forestry, Duke University, Durham, North Carolina 27706
570. R. A. Elder, TVA Engineering Laboratory, Norris, Tennessee 37828
571. D. W. Cole, College of Forest Resources, Washington University, Seattle, Washington 98105
572. D. D. Wooldridge, College of Forest Resources, University of Washington, Seattle, Washington 98105
573. K. J. Seigworth, Division of Forestry Development, Norris, Tennessee
574. R. Betson, Hydraulic Data Branch, TVA, Knoxville, Tennessee 37916
575. M. A. Churchill, Environmental Hygiene Branch, TVA, Chattanooga, Tennessee
576. H. E. Wright, Jr., Limnological Research Center, University of Minnesota, Minneapolis, Minnesota 55455
577. W. E. Sopper, School of Forestry, Pennsylvania State University, University Park, Pennsylvania 16802
578. B. J. Frederick, U.S. Geological Survey, Knoxville, Tennessee 37902
579. F. A. Gifford, Atmospheric and Turbulence Laboratory, Oak Ridge, Tennessee

580. W. M. Culkowski, Atmospheric and Turbulence Laboratory, Oak Ridge, Tennessee
581. John C. Fry, Illinois State Geological Survey, Natural Resources Building, Urbana, Illinois 61801
582. John Kadlec, School of Natural Resources, University of Michigan, Ann Arbor, Michigan 48104
583. Frederick E. Smith, School of Natural Resources, University of Michigan, Ann Arbor, Michigan 48104
584. J. E. Hubbard, Dept. of Geology and Earth Science, University College at Brockport, Brockport, New York 14420
585. P. A. Briegleb, Director, Pacific Northwest Forest and Range Experiment Station, P. O. Box 3141, Portland, Oregon 97208
586. R. D. McCulley, Director, Pacific Southwest Forest and Range Experiment Station, P. O. Box 245, Berkeley, California 94701
587. L. E. Walker, Head Librarian, College of Forestry, Syracuse University, Syracuse, New York
588. Donald Watts, Department of Statistics, University of Wisconsin, Madison, Wisconsin
589. C. F. Becker, Agricultural Engineering Section, University of Wyoming, Laramie, Wyoming 82070
590. W. L. Decker, Dept. of Atmospheric Science, College of Agriculture, University of Missouri, Columbia, Missouri 65201
591. C. C. Delwiche, Dept. of Soils and Plant Nutrition, College of Agriculture University of California, Davis, California 95616
592. Ralph L. Dix, Dept. of Botany and Plant Pathology, Colorado State University, Fort Collins, Colorado 80521
593. Josephine K. Doherty, Environmental Biology, National Science Foundation, 1800 G Street, N.W., Room 331, Washington, D. C. 20550
594. Richard C. Dugdale, Dept. of Oceanography, University of Washington, Seattle, Washington 98105
595. James J. Fuquay, Environmental and Life Sciences, Battelle-Northwest, P. O. Box 999, Richland, Washington 99352
596. A. D. Hasler, Laboratory of Limnology, University of Wisconsin, Madison, Wisconsin 53706
597. D. M. Hopkins, Office of Marine Geology and Hydrology, U.S. Geological Survey, 4 Homewood Place, Menlo Park, California 94205
598. B. H. Ketchum, Environmental Biology Program, National Science Foundation, 1800 G Street, N.W., Washington, D. C. 20550
599. C. L. Lefebvre, Plant Science Research Program, Cooperative State Research Service, U.S. Dept. of Agriculture, Washington, D. C. 20250
600. E. R. Lemon, Microclimate Investigations, SWC-ARS-USDA, Cornell University, Bradfield Hall, Ithaca, New York 14850
601. R. M. Linn, Office of Natural Science Studies, National Park Service, Interior Building, Room 1226, Washington, D. C. 20240
602. Lester Machta, Air Resources Laboratory, Environmental Science Services Administration, Gramax Building, 8060 13th Street, Silver Spring, Maryland 20910
603. W. D. McClellan, Agricultural Research Service, Plant Industry Station, USDA, Beltsville, Maryland 20705
604. J. T. Middleton, National Air Pollution Control Administration, 801 North Randolph Street, Room 906, BCT-2, Arlington, Virginia 22203

605. F. M. Morthland, Special Projects Branch, Life Sciences Division, Office of the Chief, Research and Development, U.S. Dept. of the Army, Washington, D.C. 20301
606. D. H. Pack, Air Resources Laboratory, Environmental Science Services Administration, Gramax Building, 8060 13th St., Silver Spring, Maryland
607. R. M. Paul, Land and Facilities Development Administration, Dept. of Housing and Urban Development, Washington, D.C. 20410
608. L. K. Porter, Research Soil Scientist, Agricultural Research Service, Colorado State University, Fort Collins, Colorado 80521
609. H. E. Savely, Directorate of Life Sciences, Air Force Office of Scientific Research, U.S. Dept. of the Air Force, 1400 Wilson Boulevard, Arlington, Virginia 22209
610. R. E. Scantlebury, International Scientific and Technological Affairs, U.S. Dept. of State, New State Dept. Building, Washington, D.C. 20523
611. F. L. Stone, National Institute of General Medical Sciences, National Institutes of Health, Westwood Building, Room 953, Bethesda, Maryland
612. C. B. Tanner, Dept. of Soils and Meteorology, University of Wisconsin, Madison, Wisconsin 53706
613. P. E. Waggoner, Dept. of Soil and Climatology, The Connecticut Agricultural Experiment Station, 123 Huntington Street, Box 1106, New Haven, Connecticut 06504
614. Laboratory and University Division, AEC, ORO
615-901. Given distribution as shown in TID-4500 under Health and Safety category (25 copies — CFSTI)